Chemical Geology (Isotope Geoscience Section), 73 (1988) 169-198
Elsevier Science Publishers B.V., Amsterdam — Printed in The Netherlands

FISSION-TRACK GEOCHRONOLOGY, TECTONICS AND STRUCTURE OF THE TRANSANTARCTIC MOUNTAINS IN NORTHERN VICTORIA LAND, ANTARCTICA

PAUL G. FITZGERALD* and ANDREW J.W. GLEADOW

Geology Department, University of Melbourne, Parkville, Vic. 3052 (Australia)

(Received February 25, 1987; revised and accepted March 25, 1988)

Abstract

Fitzgerald, P.G. and Gleadow, A.J.W., 1988. Fission-track geochronology, tectonics and structure of the Transantarctic Mountains in northern Victoria Land, Antarctica. Chem. Geol. (Isot. Geosci. Sect.), 73: 169–198.

A regional fission-track dating study in northern Victoria Land (NVL) provides information on the amount, timing and variable rates of uplift of the Transantarctic Mountains (TAM) at their northernmost extent. Apatite ages increase systematically with elevation and together with confined track length distributions, define a two-stage uplift history, although a variety of thermal histories, resolvable by use of confined track length distributions, exist for different parts of NVL. A pronounced "break in slope" in the apatite age-elevation profile for results from most of NVL occurs at ~50 Ma, approximating the start of uplift of the mountains. This marks the base of an uplifted apatite annealing zone. Prior to uplift, samples above this break lay within the apatite annealing zone whereas those samples below it had an apatite fission-track age of zero. For most of NVL, ~5 km of uplift have been calculated. In the southeastern coastal region, however, uplift of the order of 10 km has been estimated, exposing apatite ages of only 25–35 Ma. Sphene and zircon ages from this area also appear reduced relative to the regional pattern, suggesting that the partial annealing zones for these minerals have been revealed. Confined track length distributions from the lower part of the apatite age profile indicate an initially rapid period of uplift (~200–400 m Ma^{-1}) from ~50 Ma. In the Lichen Hills–Outback Nunataks area, in the west of NVL, apatites have not been completely overprinted by the Jurassic thermal event associated with emplacement of the Ferrar Dolerite, and uplift here is of the order of only 4 km. Block faulting associated with uplift of the TAM is considered to be the same event as Rennick Faulting leading to the formation of the Rennick Graben.

1. Introduction

North Victoria Land (NVL) marks the extreme northwestern end of the Transantarctic Mountains (TAM) in the Ross Sea Sector of Antarctica (Fig. 1). This spectacular and majestic mountain range with many peaks over 4000 m above sea-level (a.s.l.) stretches from the Pensacola Mountains in the Weddell Sea region for ~3500 km until it terminates on the Pacific coast of NVL. The TAM naturally divides Antarctica into two separate and distinct geological provinces, the Precambrian craton of East Antarctica and the West Antarctic mobile belts of dominantly Mesozoic–Cenozoic age. The tectonic relationship between these two provinces remains one of the outstanding problems of Gondwana geology (Dalziel and Elliot, 1983). In NVL the TAM are at their widest,

**Present address*: Geology Department, Arizona State University, Tempe, AZ 85287, U.S.A.

0168-9622/88/$03.50

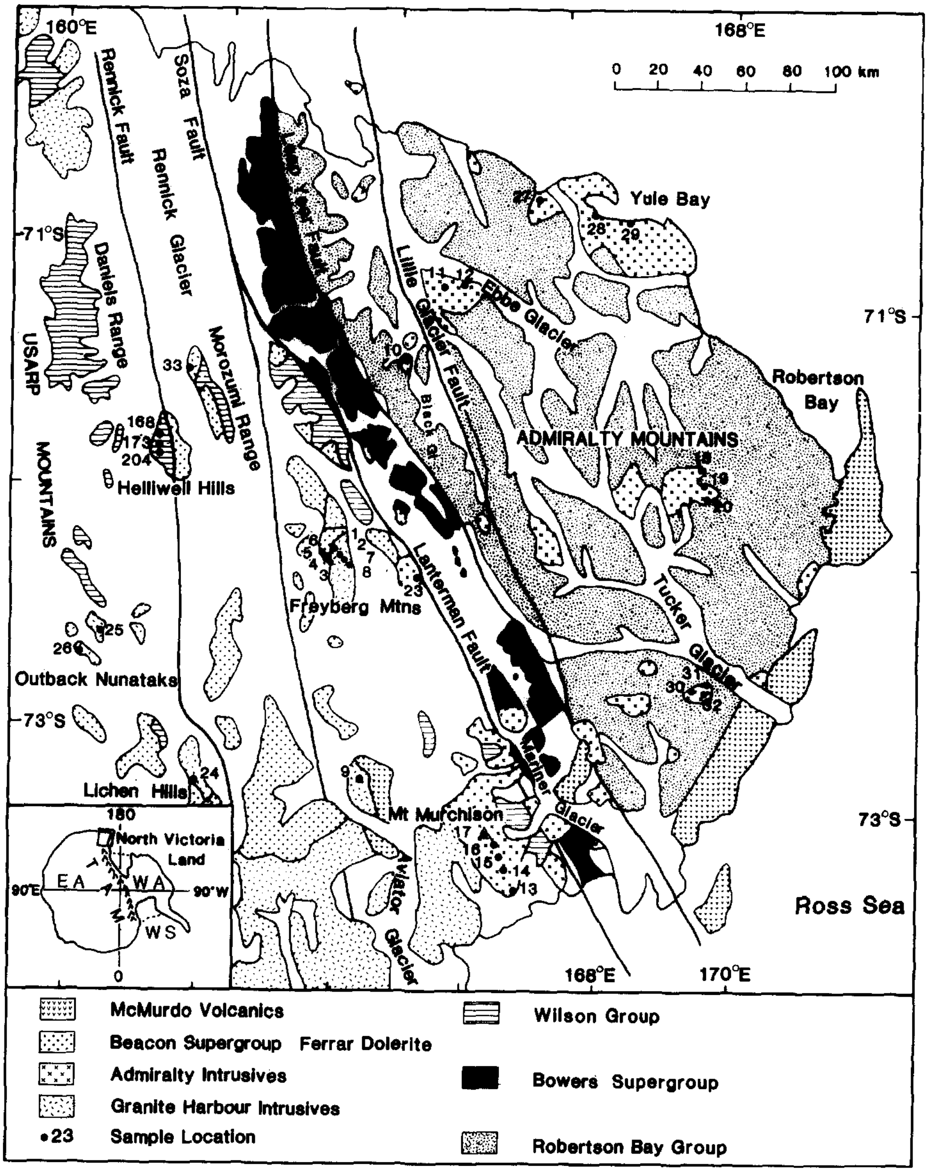

Fig. 1. Geological map of northern Victoria Land showing the three major late Precambrian–early Palaeozoic terranes (Wilson, Bowers and Robertson Bay Groups), the Cambro-Ordovician Granite Harbour and Devonian Admiralty Intrusives, and sample localities. Also shown are the Permo-Carboniferous to Triassic Beacon Supergroup and Jurassic Ferrar Dolerite (including the Kirkpatrick Basalt). Geology is after Gair et al. (1969), Bradshaw and Laird (1983) and Bradshaw et al. (1985). Sample numbers are shown as the final two digits from the form *R317--*, except for the three samples from the Helliwell Hills which are given as the final three digits from the form *R32---*. Abbreviations within the inset map are as follows: *WA* = West Antarctica; *EA* = East Antarctica; *WS* = Weddell Sea.

being ~400 km in width compared to an average 100–300 km in other parts of the range. It also represents the most complete surface exposure through the mountains, but it is not a representative cross-section of the entire TAM. The eastern bulge (Fig. 1) of NVL protruding into the Ross Sea is unique along the length of the TAM and contrasts with the usually smooth Ross Sea coastline. The highest peaks in NVL lie within this eastern bulge closest to the Ross

Sea, and reach elevations of 4000 m a.s.l. in the Admiralty Mountains. From here, the summit heights decrease sharply to the coast but towards the west the decrease is more gradual, eventually reaching a low in the Rennick Glacier depression. West of here, the fault block of the Usarp Mountains with elevations of ~2000 m a.s.l. forms a barrier against the ice of the polar plateau.

The aim of this paper is two-fold: (1) to present fission-track data from the NVL region of Antarctica with a view to determining and interpretating the uplift history of that area; and (2) to show the use of confined fission-track length distributions in the interpretation of different thermal histories and hence their application to uplift studies.

The fieldwork for this study was undertaken as part of the 1981/1982 International North Victoria Land Expedition (Stump et al., 1982a). Samples were collected from the basement rocks of NVL from a helicopter supported base-camp located on the Evans Neve, near the Freyberg Mountains (72°12′S, 163°50′E). This was done in cooperation with another study examining the early to middle Palaeozoic granitic rocks of NVL (Stump et al., 1982b).

2. Apatite uplift studies

Apatite fission-track dating has been applied to the study of uplift histories of mountain belts since the observation that apatite fission-track ages increase with increasing elevation (Dodge and Naeser, 1968; Wagner and Reimer, 1972). This pattern has been explained as a consequence of a rock column moving upwards through an idealized critical isotherm for fission-track retention in apatite (or closure temperature) during the uplift and erosion leading to mountain formation. The effective closure temperature is notionally equivalent to the stage at which approximately half the number of fission tracks become stable (Wagner and Reimer, 1972; Wagner et al., 1977), and varies with the cooling rate (Wagner and Reimer, 1972; Dodson, 1973; Haack, 1977; Wagner et al., 1977). The principle of a simple closure temperature in apatite has been applied in many previous studies to constrain the cooling histories and "uplift and erosion" rates in the Alps of central Europe (Schaer et al., 1975; Wagner et al., 1977; Hurford, 1986), the Himalayas (Zeitler et al., 1982), the Andes (Nelson, 1982; Kohn et al., 1984a, b; Shagam et al., 1984), the Sinai Pensinsula (Kohn and Eyal, 1981), the Coast Range of British Columbia (Parrish, 1983) and to various ranges within the western Cordillera of the U.S.A. (Naeser, 1979; Bryant and Naeser, 1980; Naeser et al., 1983; Kelley and Duncan, 1986).

Fission tracks in apatite anneal when subject to quite low temperatures over geological time. For cooling rates of 0.1–100°C Ma^{-1} over periods of 10–100 Ma the effective closure temperature for apatite is ~100±20°C (Naeser and Faul, 1969; Calk and Naeser, 1973; Zimmerman, 1977; Harrison et al., 1979). Using this principle of simple closure temperatures it has proved possible to calculate "uplift and erosion" rates by one of three methods:

(1) The gradient of apatite fission-track age plotted against sample elevation is taken to be the apparent "uplift rate" over the period given by the apatite ages. Wagner et al. (1977) were the first to undertake a comprehensive study along these lines when they examined the uplift histories of different regions of the Alps. Other examples are given by Miller and Lakatos (1983), Gleadow et al. (1984), Kohn et al. (1984a), Shagam et al. (1984), and Kelley and Duncan (1986).

(2) By extrapolation of an apatite fission-track age from the sample elevation to its estimated depth of zero age, assuming a geothermal gradient or using a measured geothermal gradient. For example, an apparent uplift rate can be calculated from a sample taken from an elevation of 1000 m having an age of 100 Ma. Assuming a geothermal gradient of 25°C km^{-1} gives a depth to zero apatite age of 4 km, which implies a minimum uplift rate for the area in

question of 50 m Ma^{-1} (e.g., Wagner et al., 1977; Kohn and Eyal, 1981; Miller and Lakatos, 1983; Crowley et al., 1985).

(3) Using different closure temperatures from different minerals in the same isotopic system (e.g., apatite and zircon fission-track pairs) or different isotopic systems to determine a cooling rate and dividing this by the geothermal gradient to give an "uplift" rate (e.g., Wagner et al., 1977; Gleadow and Brooks, 1979; Harrison et al., 1979; Nelson, 1982; Parrish, 1982; Zeitler et al., 1982; Kohn et al., 1984b; Zeitler, 1985; Hurford, 1986; Mailhe et al., 1986).

These three methods all assume constant geothermal gradients with time and do not take into account any variable uplift rates, the rising of critical isotherms during a tectonic event or relaxation of those isotherms after that event, variations in radioactive heat generation or changes in the geothermal regime as a result of tectono-magmatic processes.

Parrish (1982, 1983) called the apatite age–sample elevation gradient the "apparent uplift rate"; which he defined as:

> "the rate at which the critical isotherm (approximately 100°C) moved downward with respect to the rock column".

This is equivalent to the "apparent denudation rate" of Kelley and Duncan (1986).

According to Parrish (1982, 1983) the "apparent uplift rate" will equal the true uplift rate when the following conditions are met:

(1) Critical isotherms must have been horizontal and uninfluenced by surface topography or variable thermal conductivity.

(2) Critical isotherms must remain at a constant depth with respect to the surface, regardless of uplift rate.

(3) Uplift must be equal to erosion.

With relevance to fission-track studies, Parrish (1985) concluded:

(1) That these conditions are likely to be met and true "uplift and erosion" rates approximately equal to apparent rates provided they do not exceed 300 m Ma^{-1}.

(2) Uplift at rates in excess of 500 m Ma^{-1} produces a profound disturbance upon isotherms and geothermal gradients.

(3) Thermal relaxation can cause erroneous estimates of true uplift rates, but apatite age–elevation derived rates are considerably more accurate than those based on other dating methods with higher closure temperatures.

(4) After the first few million years of rapid uplift, uplift and erosion can be considered to be in equilibrium, requiring no additional correction. For periods of very recent rapid uplift, apparent rates must be treated with caution.

Advances in the understanding of apatite fission-track annealing have shown that annealing takes place over a range of temperatures (Naeser, 1979; Gleadow and Duddy, 1981; Gleadow et al., 1983; Green et al., 1988). In essence this means that it is simplistic to talk in terms of a single closure temperature for apatite fission-track retention. The annealing temperature range has been defined as the "partial stability zone" (Wagner, 1972) or the "partial annealing zone". We refer to it here simply as the annealing zone. Gleadow and Duddy (1981) found that the apatite annealing zone for the Otway Basin of southeastern Australia lay between the temperatures of 70° and 125°C.

Green et al. (1985, 1986) show that annealing is occurring all the time even at ambient surface temperatures and that as soon as a fission track is formed, it is in an "annealing environment". The annealing rate at different temperatures varies with time; at surface temperatures it is very slow and at temperatures hotter than the base of the annealing zone it is essentially instantaneous. Therefore, the concept of a discrete apatite annealing zone, although not strictly valid, is still a useful idea and refers to a zone of "accelerated annealing" above the base of the annealing zone.

Green et al. (1986) show that the annealing temperature range is dependent to a certain extent on the chemical composition of the apatite, in particular the Cl/F ratio. Chlorapatites retain tracks at higher temperatures than do fluorapatites. The apatites from the Otway Basin have a range of chemical composition (Green et al., 1985) which means that the temperature range defining the annealing zone is broader than if the apatites were monocompositional (Gleadow and Duddy, 1981; Green et al., 1986). Otway Basin apatites include compositions that are more chlorine rich than apatites from most granitic rocks which tend to be fluorapatites (Fershtater et al., 1984). Therefore the base of the apatite annealing zone in the Otway Basin lies at a higher temperature than it would if the apatites were fluorine rich. A more realistic annealing temperature range for granitic apatites with a lower Cl/F ratio is therefore estimated to be ~60–100°C. Gleadow and Fitzgerald (1987) used an apatite annealing temperature interval of 70–125°C in their study of uplift of the TAM in southern Victoria Land.

It is critical in any apatite fission-track uplift study to correctly determine that an apatite age–elevation gradient actually represents an "apparent uplift rate" and has not been imparted by processes unrelated to uplift and erosion. Within an apatite annealing zone, fission-track ages increase from zero at the base of the annealing zone up to a finite age at the top of the annealing zone. This upper age is governed by the previous thermal and tectonic history of an area and in the case of sedimentary basins will be at least the depositional age. Therefore, there exists within the annealing zone a gradient defined by this finite age change over a temperature interval. This apatite age gradient is dependent on two variables, the vertical thickness of the annealing zone (dependent on the geothermal gradient and to some extent the compositional variation) and the age of the apatites at the top of the annealing zone (dependent on the previous history). This apparent apatite age gradient is therefore a function of the thermal history of that geologic terrain. Should that terrain subsequently undergo a period of rapid uplift, the annealing zone will be uplifted and may be preserved in the rock column. The gradient of such an "uplifted" annealing zone *will not* represent an "apparent uplift rate". It is instead a relict of a fossil apatite annealing zone that formed prior to uplift. Uplift will be recorded in the samples that lie beneath the base of the annealing zone that had an apatite age of zero prior to uplift. Such uplifted annealing zones have been identified in the Rocky Mountains in North America (Naeser, 1979; Bryant and Naeser, 1980) and also in the TAM of southern Victoria Land (Fitzgerald, 1986; Gleadow and Fitzgerald, 1987).

Thus there are two interpretations for an apatite age–elevation gradient. It may represent an "apparent uplift rate" or alternatively an "uplifted annealing zone". The ability to distinguish between the two cases is critical and fundamental in any fission-track uplift study. The question then remains as to how these two alternatives can be distinguished. The distribution of confined fission-track lengths is critical in this respect.

The principles of the interpretation of confined fission-track length distributions in apatite have recently been examined by Gleadow et al. (1986a, b) and Green et al. (1988). Apatite age is reduced during annealing largely as the result of the reduction in the etchable range of fission tracks and since this is revealed in the length of confined fission tracks, track length is a more fundamental source of palaeotemperature information (Gleadow et al., 1983). These studies show that in rapidly cooled rocks such as surficial volcanics or rapidly uplifted terrains which have not been heated above ~50°C subsequent to their original cooling, the fission-track length distribution is narrow (a standard deviation of ±1 μm), with most tracks between 13 and 16 μm and a mean of 14–15 μm. Apatites that were initially zero in age and then rapidly uplifted to near-surface levels would have volcanic-type length distributions. Apatite which has any other sort of length distribution therefore reflects a more complex thermal history. The length reduction of a track is dependent upon the maximum temperature it has experienced throughout its existence. Tracks are produced continuously throughout time and so the shortest tracks have experienced higher temperatures and longer tracks (13–16 μm) have not experienced temperatures significantly in excess of $\sim 20\,^{\circ}$C. The relative proportions of long and short tracks in a length distribution can therefore reveal the relative proportions of time that a sample has resided at various temperatures, and it is this principle that has been applied to determining the various thermal histories in NVL.

3. Geology of northern Victoria land

The late Precambrian–early Palaeozoic basement geology of NVL (Fig. 1) has traditionally been divided into three distinct units (Gair et al., 1969; Sturm and Carryer, 1969; Tessensohn et al., 1981), although recently Bradshaw et al. (1985) have defined five suspect terranes. The metasedimentary basement units consist of the Robertson Bay Group to the east, the Bowers Supergroup in the central part and the Wilson Group to the west, and are separated by major NW–SE-trending faults. The Robertson Bay Group is a lower Palaeozoic sequence of quartz-rich turbidites (Wright, 1981; R.A. Cooper et al., 1983). The Bowers Supergroup (Bradshaw and Laird, 1983), of early Palaeozoic age consists of volcanics with intercalated sediments. This terrane is bounded by the Lanterman Fault Zone to the west (Bradshaw et al., 1982) and is characterised by folds and faults oriented subparallel to the Leap Year Fault to the east (Bradshaw et al., 1985). The high-grade metamorphic Wilson Group of probable late Precambrian age (Kreuzer et al., 1981; Adams et al., 1982) consists of gneisses and metasediments.

Two suites of granites have intruded the metasedimentary units described above. These are the Cambro-Ordovician Granite Harbour Intrusive Suite and the Devonian Admiralty Intrusives. The Granite Harbour Intrusives intrude the Wilson Group and include a variety of syn- to post-tectonic granites and migmatites. To the southwest of the Wilson Group these granites have characteristics typical of S-types (Chappell and White, 1974), whereas along the northeastern margin of this area there are more mafic tonalites and granodiorites. Around the Aviator Glacier these granites have more of an I-type affinity. The Admiralty Intrusives intrude the Robertson Bay Group and Bowers Supergroup. These are all high-level contact aureole types with no clearly defined S-types being present (Stump et al., 1986), and have the form of discordant plutons (Grindley and Oliver, 1983).

The basement rocks of NVL are overlain by Permo-Carboniferous glacigene and Permo-Triassic coal-bearing alluvial plain sediments of the Beacon Supergroup (Laird and Bradshaw, 1981; Walker, 1983). These strata rest unconformably on an erosion surface of subdued relief called the "Sub-Beacon Peneplain" by Gair (1967) and the "Sub-Beacon Surface" by Dow and Neall (1974). Structurally the Beacon Supergroup is either horizontal or tilted up to 10° and divided into blocks in the order of 10 km across (Walker, 1983). In the Freyberg Mountains, Walker (1983) traced the Sub-Beacon Surface for ~ 5 km dipping 5° west. At the Helliwell Hills the sequence is tilted $\sim 5^{\circ}$ east and in the Morozumi Range, $\sim 5^{\circ}$ west (Sturm and Carryer, 1969). In the lower Rennick Glacier the Beacon displays a persistent but gentle dip to the west and southwest (Dow and Neall, 1974) and in the upper Rennick Glacier Gair (1967) noted a regional dip of 2–3° to the northwest. The Beacon Supergroup in NVL is only 300 m thick, in contrast to the sequence up to 3 km thick in the central TAM and southern Victoria Land where it is also older (Devonian to Triassic; Barrett et al., 1972).

Deposition of Beacon sediments was followed by a period of Early–Middle Jurassic tholeiitic magmatism, resulting in the extrusion of the Kirkpatrick Basalts and intrusion of the Ferrar Dolerite. The basalts are up to 2 km thick in the upper Rennick Glacier (Gair, 1967) and at Litell Rocks east of the Morozumi Range (Tessensohn et al., 1981). The Ferrar Dolerite occurs mainly as sills but also as cross-cutting dykes. Kyle et al. (1983), using the $^{40}Ar/^{39}Ar$ method, dated dolerites at 163–179 Ma and basalts at 176–184 Ma. A 160-Ma gap exists in the onland geological record between tholeiitic magmatism and extrusion of Cenozoic alkaline basalts of the McMurdo Volcanic Group, which occur near the Ross Sea coast. Kreuzer et al. (1981) dated rocks of the McMurdo Volcanic Group that ranged from 13 to 1 Ma. Minor Tertiary granites have also been found in the Mariner Glacier area (Stump et al., 1983).

The tectonic history of NVL has been the subject of some debate over the last five years (Bradshaw and Laird, 1983; Grindley and Oliver, 1983; Weaver et al., 1984; Bradshaw et al., 1985; Gibson and Wright, 1985), especially with regard to the relationships between the pre-Palaeozoic terranes. The Ross Orogeny in NVL incorporates events of late Precambrian to Early Ordovician in age (Bradshaw and Laird, 1983) and in its later stages is dominated by intrusion of the Granite Harbour igneous suite and deformations relating to the accretion of the Robertson Bay terrane onto the Antarctic continent (Gibson, 1985). Tholeiitic magmatism in the Jurassic has been related to the initial fragmentation of Gondwana (Kyle et al., 1981) and was accompanied by widespread heating which in southern Victoria Land resulted in complete annealing of fission tracks in apatite.

The period of tectonic history that concerns this contribution involves the formation of the TAM. This has been traditionally regarded as a block-faulting event of Cenozoic age (Brady and McKelvey, 1979; Denton, 1979; Webb, 1979; Katz, 1982) and was defined as the Victoria Orogeny by Gunn and Warren (1962). Gleadow and Fitzgerald (1987) using fission-track dating in southern Victoria Land have shown that the initiation of uplift of the TAM was of early Tertiary age.

Tessensohn et al. (1981) recognize two main block-faulting events in NVL. The Bowers event brought blocks of different metamorphic grade into juxtaposition, was deep-seated and had major throws. The best example of this event is the Bowers Structural Zone where the western high-grade Lanterman block is upthrown against the Bowers Graben filled with low-grade metasediments to the east. The timing of this event is after the Cambro-Ordovician Ross Orogeny but prior to intrusion of the Devonian Admiralty Intrusives (Tessensohn, 1984) and so was not responsible for the present TAM.

A second phase of block faulting offsetting the base of the Beacon Supergroup at least several hundred metres vertically is seen in the Rennick Glacier region (Dow and Neall, 1974). This post Beacon/Ferrar block faulting was termed Rennick Faulting by Tessensohn et al. (1981). A northward extension of the Rennick Fault (Gair, 1967) can be seen in the Helliwell Hills (Sturm and Carryer, 1969) where the west side has been differentially upthrown 600 m. Reactivation of old Bowers faulting structures has been reported in the upper Black Glacier where Beacon sediments and Ferrar Dolerite are displaced along boundary faults of the Bowers Structural Zone (Tessensohn et al., 1981). The Lanterman Range which is fault bounded on both sides exposes evidence for complex post-Jurassic deformation in the form of four intensely infaulted and infolded Beacon/Ferrar inliers (Grindley and Oliver, 1983). The intensity of deformation of these synclines in the Beacon Supergroup is unusual and led Grindley and Oliver (1983) to imply compressional (-strike-slip) movements rather than simple normal faulting.

The timing of the Rennick block faulting is clearly post-Jurassic because Ferrar Dolerite is involved. However, it is not clear whether this phase was contemporaneous with Cenozoic rifting in the Ross Embayment and/or uplift of

TABLE I

Analytical results, apatite fission ages from the basement rocks of North Victoria Land

Sample No.	Locality	Elevation (m a.s.l.)	Number of grains	Standard track density (10^6 cm^{-2})	Fossil track density (10^6 cm^{-2})	Induced track density (10^6 cm^{-2})	Correlation coefficient	χ^2 probability (%)	Age (Ma)	U (ppm)
R31701	Freyberg Mountains	1,870	12	1.24 (8,263)	1.485 (1,037)	3.931 (2,745)	0.929	18	82 ± 3	41
R31702	Freyberg Mountains	1,870	11	1.24 (8,263)	2.639 (1,898)	7.079 (5,092)	0.757	< 1	81 ± 2, 86 ± 7*	74
R31703	Freyberg Mountains	1,895	20	1.24 (8,263)	0.848 (616)	2.338 (1,698)	0.868	10	79 ± 4	26
R31704	Freyberg Mountains	1,815	18	1.24 (8,263)	0.826 (1,040)	2.113 (2,662)	0.956	14	85 ± 3	22
R31705	Freyberg Mountains	1,694	14	1.24 (8,263)	1.049 (920)	2.884 (2,529)	0.987	93	79 ± 3	32
R31706	Freyberg Mountains	1,532	20	1.24 (8,263)	0.930 (734)	3.068 (2,422)	0.886	15	66 ± 3	33
R31707	Freyberg Mountains	1,950	14	1.24 (8,263)	2.133 (740)	5.892 (2,044)	0.935	9	79 ± 4	63
R31708	Freyberg Mountains	1,988	10	1.24 (8,263)	1.422 (1,221)	4.191 (3,598)	0.779	< 1	74 ± 3, 74 ± 4*	46
R31709	Aviator Glacier	1,015	20	1.24 (8,263)	0.669 (992)	3.310 (4,907)	0.971	96	44 ± 2	38
R31710	Copperstain Ridge, Lillie Glacier	945	17	1.24 (8,263)	0.419 (134)	1.873 (599)	0.919	70	49 ± 5	19
R31711	Ebbe Glacier	690	17	1.24 (8,263)	0.621 (721)	3.608 (4,192)	0.689	8	37 ± 2	37
R31712	Mt. Craven, Ebbe Glacier	1,160	16	1.24 (8,263)	0.684 (568)	3.345 (2,779)	0.954	25	44 ± 2	36
R31713	Mt. Murchison	5	14	1.35 (11,423)	0.254 (138)	2.225 (812)	0.946	93	27 ± 3	21
R31714a	Mt. Murchison	1,345	18	1.35 (11,423)	1.283 (563)	11.22 (4,924)	0.884	67	27 ± 1	109
R31714b			15	1.35 (11,423)	1.357 (359)	12.67 (3,353)	0.860	30	25 ± 2	123
R31715a	Mt. Murchison	1,690	13	1.34 (11,423)	0.258 (161)	2.289 (1,428)	0.882	48	27 ± 2	21
R31715b			17	1.34 (11,423)	0.192 (189)	1.464 (1,443)	0.953	51	31 ± 2	14
R31716a	Mt. Murchison	2,715	15	1.33 (11,423)	0.204 (108)	1.379 (731)	0.732	34	35 ± 4	14
R31716b			16	1.33 (11,423)	0.208 (110)	1.364 (722)	0.621	33	36 ± 4	14
R31717a	Mt. Murchison	3,385	20	1.32 (11,423)	0.544 (369)	4.197 (2,846)	0.874	30	30 ± 2	41
R31717b			19	1.32 (11,423)	0.521 (227)	4.132 (1,799)	0.516	8	29 ± 2	40

R31718	Mt. Royalist	3,445	16	1.32 (11,423)	1.758 (607)	3.245 (1,120)	0.917	46	125±6	32
R31719a	Mt. Ajax	3,650	16	1.31 (11,423)	0.781 (221)	1.679 (475)	0.880	81	106±9	18
R31719b			11	1.31 (11,423)	0.809 (168)	1.869 (388)	0.500	23	99±9	21
R31720	Mt. Royalist	2,200	18	1.57 (5,508)	0.542 (217)	1.968 (788)	0.790	70	76±6	16
R31723	Salamander Range	2,370	18	1.22 (10,675)	0.472 (198)	1.239 (520)	0.904	97	81±7	14
R31724a	Section Peak, Lichen Hills	2,085	11	1.36 (11,790)	4.836 (2,028)	3.734 (1,566)	0.990	90	304±11	34
R31724b			14	1.37 (7,701)	4.711 (1,882)	3.602 (1,439)	0.965	21	315±11	33
R31725	Mt. Spatz, Outback Nunataks	2,325	12	1.15 (2,193)	2.756 (1,169)	2.771 (1,175)	0.910	2	199±9, 196±12*	32
R31726	Miller Butte, Outback Nunataks	2,731	11	1.15 (2,193)	3.730 (1,174)	3.130 (985)	0.934	4	238±12, 251±17*	36
R31727	McMahon Glacier	145	18	1.22 (10,675)	0.291 (223)	1.921 (1,474)	0.942	96	32±2	22
R31728a	Yule Bay	25	10	1.29 (11,423)	0.359 (137)	1.901 (726)	0.916	84	43±4	20
R31728b			18	1.29 (11,423)	0.269 (192)	1.551 (1,109)	0.781	4	39±3, 42±5*	16
R31729	Yule Bay	45	19	1.29 (11,423)	0.572 (514)	2.610 (2,344)	0.881	1	50±3, 48±3*	28
R31730	Oread Spur, Lower Tucker Glacier	2,145	15	1.28 (11,423)	1.190 (444)	7.875 (2,939)	0.972	49	34±2	77
R31731	Mt. Northampton	175	18	1.27 (11,423)	0.172 (124)	1.576 (1,136)	0.654	73	24±2	12
R31732	Mt. Northampton	1,530	21	1.26 (11,423)	0.274 (145)	1.760 (933)	0.831	34	34±3	16
R31733	Morozumi Range	700	22	1.22 (10,675)	0.408 (441)	2.076 (2,243)	0.931	80	42±2	20
R32168	Helliwell Hills	1,500	21	1.33 (9,313)	0.194 (202)	0.453 (471)	0.713	26	100±9	4
R32173	Helliwell Hills	1,450	21	1.33 (9,313)	0.812 (418)	1.941 (998)	0.919	8	98±6	20
R32204	Helliwell Hills	1,550	18	1.33 (9,313)	1.662 (1,015)	3.894 (2,378)	0.986	56	100±4	37

Brackets show number of tracks counted. Standard and induced track densities measured on mica external detectors ($g=0.5$), and fossil track densities on internal mineral surfaces. Ages calculated using $\zeta=354$ for dosimeter glass SRM612 (Hurford and Green, 1983).

*Mean age, used where pooled data fail χ^2-test at 5%.

the TAM. On the other hand, some movement has been proposed in the Cretaceous because Jurassic dolerite and basalt at Litell Rocks have Early Cretaceous K–Ar ages (Kreuzer et al., 1981), which suggests they have been reset and led Grindley and Oliver (1983) to suggest some fault-block movement at this time. The presence of mountains 3–4 km in height with a young morphology led both Tessensohn et al. (1981) and Grindley and Oliver (1983) to believe there had been movement some time in the Cenozoic.

4. Methods

4.1. Fission-track ages

Samples of basement rocks ~2 kg in weight were crushed and the apatites separated using conventional heavy-liquid and magnetic techniques. The apatites were mounted in epoxy resin on glass slides, ground to reveal an internal surface, polished, and then etched for 20 s in 5 *N* HNO_3 at 20°C to reveal fossil fission tracks. Zircons were mounted in Teflon®, ground, polished and then etched for periods up to 106 hr. in a KOH–NaOH eutectic melt at 215°C (Gleadow et al., 1976) to reveal fossil fission tracks and then cleaned in 40% HF for 4 hr. at 20°C. Sphenes were mounted in epoxy, ground, polished and then etched to reveal tracks in 50 *N* NaOH at 125°C for 30–40 min. Fission-track ages were measured by the external detector method using muscovite to record induced tracks (Gleadow, 1981). The muscovite detectors were etched for 20 min. in 40% HF at 20°C to reveal the induced tracks. Neutron irradiations were carried out in the X-7 position of the Australian Atomic Energy Commission HIFAR Research Reactor which has a well-thermalised flux (Cd ratio for Au ~125). Thermal neutron fluences were monitored by recording the track density in a muscovite detector attached to discs of the N.B.S. reference glass SRM*612* for apatites, U*3* glass for zircons and CN*1* glass for sphenes.

The mounts were counted at a magnification of 1250×, under a dry 80× objective, and only apatite, zircon or sphene grains displaying sharp polishing scratches were counted (Gleadow and Lovering, 1978; Gleadow, 1981). For apatites, ~20 grains in each age determination were counted whenever possible. Smaller numbers of sphene and zircon grains were counted due to the higher track densities. Ages were calculated using the zeta calibration method, following the procedures of Hurford and Green (1983) and Green (1985). Errors were calculated using the "conventional method" (Green, 1981) and are quoted at the level of one standard deviation throughout. The counting parameters used are shown at the bottom of Tables I and II; zeta calibrations of 353 for glass SRM*612* (P.G. Fitzgerald, unpublished data), 87.9 for glass U*3* (Green, 1985) and 123 for CN*1* glass (A.J.W. Gleadow, unpublished data) have been determined empirically by counting a set of carefully selected age standards in direct comparison with the K–Ar dates for these standards. The reported fission-track ages are therefore independent of uncertainties in the ^{238}U fission decay constant and eliminates the need for explicit thermal neutral dosimetry (Hurford and Green, 1982). Sample elevations were measured barometrically as described by Gleadow et al. (1984).

4.2. Track length measurements

Track lengths were measured in apatites using "confined" fossil fission tracks. These are tracks which do not intersect the polished internal surface of the apatite grain but have been etched out through fractures or other tracks that do intersect the surface (TINCLES and TINTS of Lal et al., 1969). Only horizontal confined tracks were measured, a track being taken to be horizontal if it remained in sharp focus along its length or had a bright reflection in reflected light. Horizontal tracks alone give the best representation of the track length distribution within a sample (Laslett et al., 1984). Only fully-etched tracks in grains whose polished

TABLE II

Analytical results - NVL zircons and sphenes

Sample No.	Locality	Elevation (m a.s.l.)	Number of grains	Standard track density (10^6 cm^{-2})	Fossil track density (10^6 cm^{-2})	Induced track density (10^6 cm^{-2})	Correlation coefficient	χ^2 probability (%)	Age (Ma)	U (ppm)
Zircons:										
R*31713*	Mt. Murchison	5	10	1.186 (2,592)	5.107 (1,678)	9.498 (3,121)	0.843	<1	28 ± 1, 28 ± 2*	424
R*31714*	Mt. Murchison	1,345	6	1.459 (3,067)	17.52 (1,919)	5.479 (600)	0.986	4	202 ± 10, 220 ± 16*	199
R*31717*	Mt. Murchison	3,385	6	1.459 (3,067)	18.02 (1,563)	4.531 (393)	0.949	30	250 ± 15	164
R*31731*	Mt. Northampton	175	8	1.459 (3,067)	20.31 (2,169)	5.600 (598)	0.386	<1	229 ± 11, 237 ± 33*	203
Sphenes:										
R*31711*	Ebbe Glacier	690	8	3.092 (6,390)	2.522 (2,282)	1.338 (1,211)	0.992	90	349 ± 13	17
R*31712*	Mt. Craven, Ebbe Glacier	1,160	8	3.119 (6,390)	16.70 (2,056)	8.369 (1,030)	0.701	23	372 ± 15	105
R*31713*	Mt. Murchison	5	7	3.130 (6,390)	1.574 (578)	8.282 (3,041)	0.952	<1	37 ± 2, 40 ± 3*	103
R*31717*	Mt. Murchison	3,385	8	3.145 (6,390)	14.08 (2,141)	7.511 (1,142)	0.706	2	353 ± 14, 353 ± 20*	93
R*31723*	Salamander Range	2,370	9	3.158 (6,390)	9.011 (1,631)	4.878 (883)	0.719	40	349 ± 15	60
R*31727*	McMahon Glacier	145	8	3.163 (6,390)	12.83 (1,579)	7.060 (869)	0.955	60	344 ± 15	87
R*31731*	Mt. Northampton	175	8	3.169 (6,390)	17.03 (1,603)	10.77 (1,014)	0.989	60	301 ± 13	132
R*31732*	Mt. Northampton	1,530	8	3.172 (6,390)	21.56 (1,561)	13.44 (973)	0.931	95	306 ± 13	165

Brackets show number of tracks counted. Standard and induced track densities measured on mica external detectors (g=0.5), and fossil track densities on internal mineral surfaces. Zircon ages calculated using ζ=87.9 for dosimeter glass U*3* and sphene ages ζ=123 for dosimeter glass CN*1* (Hurford and Green, 1983).
*Mean age, used where pooled data fail χ^2-test at 5%.

surfaces were approximately parallel to the *c*-axis were measured. Measurements were made under a 80× dry objective using a projection tube and digitizing tablet attached to a microcomputer. Whenever possible 100 track length measurements per sample were made, the number being less only when insufficient suitable tracks were present in the available apatite.

5. Results

Apatite results are given in Table I for 34 localities and are shown in Fig. 1 according to sample number and in Fig. 2 according to fission-track age. All samples come from either the Granite Harbour Intrusives or the Admiralty Intrusives except the three samples from the Helliwell Hills which are biotite-gneisses of the Wilson Group. Some apatites were dated twice (R*31714-17*, *-19*, *-24* and *-28*). Three zircon ages were also determined from the southeastern coastal area and 8 sphene ages (Table II), all from granites mapped as the Admiralty Intrusives.

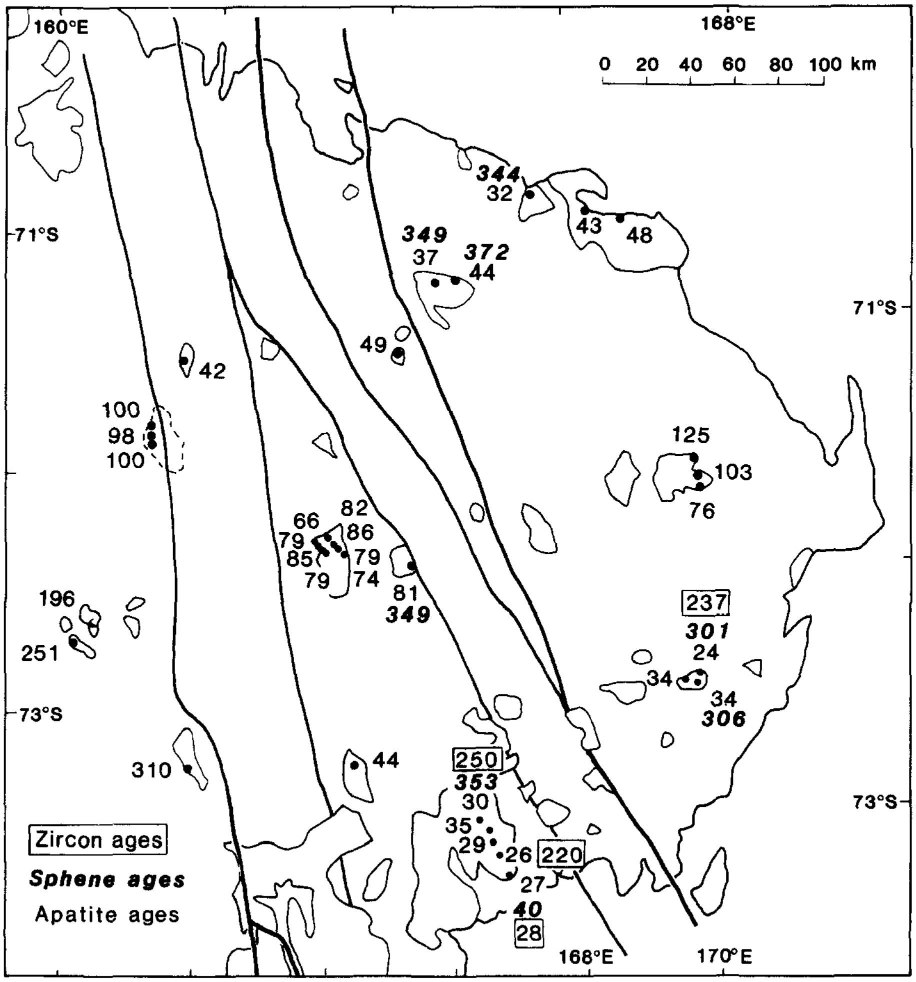

Fig. 2. Map of north Victoria Land showing outline of the granite plutons, apatite, zircon and sphene fission-track results (Ma).

5.1. Apatite fission-track ages

When plotted with respect to sample elevation (Figs. 3 and 4) the apatite ages fall into a number of well-defined patterns:

(1) The majority of apatite fission-track ages define a pattern (Fig. 3) remarkably similar to that established for southern Victoria Land (Gleadow et al., 1984; Fitzgerald, 1986; Gleadow and Fitzgerald, 1987). That this pattern is reasonably well constrained, is surprising considering the large area of the central and northern part of NVL over which these samples were collected, compared to those from southern Victoria Land.

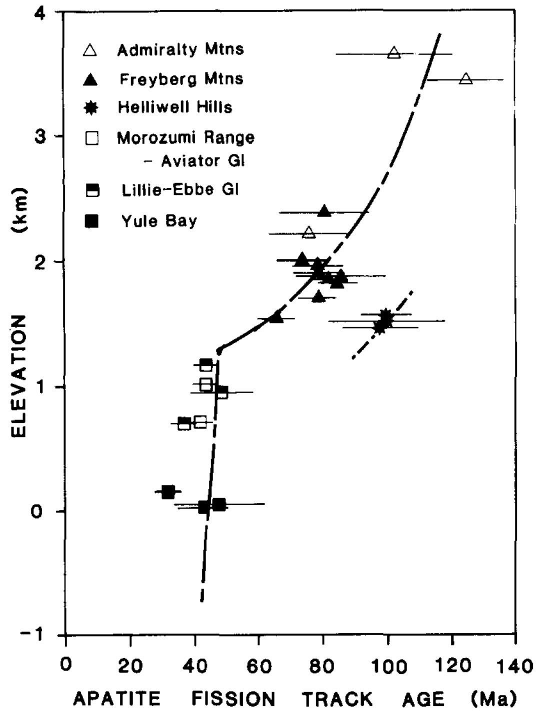

Fig. 3. Apatite fission-track results for samples from the central and northern part of NVL plotted against sample elevation. *Error bars* are two standard deviations. These define the "regional" pattern consisting of a two-stage uplift history; the "break in slope" in the apatite-age profile at ~50 Ma marking the base of the uplifted apatite annealing zone and the time of initiation of uplift of the TAM. Samples above this "break" lay in the annealing zone prior to uplift and now have mixed ages comprising an earlier set of partially annealed tracks and a later set of tracks accumulated subsequent to uplift. Samples lying below the "break in slope" had ages of zero prior to uplift and only started accumulating tracks once they were uplifted above the base of the annealing zone. Note the Helliwell Hills results lying ~1 km below the "regional" pattern, indicating they lie at a lower structural level.

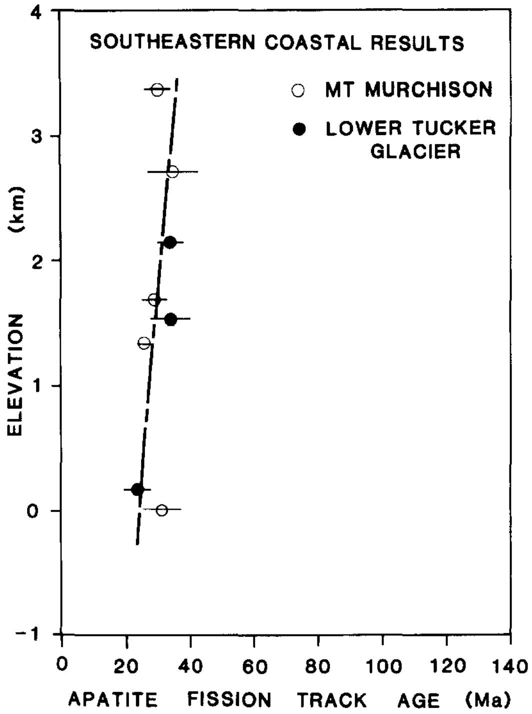

Fig. 4. Apatite age plotted against sample elevation for the southeastern coastal region samples (*R31713-17, R31730-32*). *Error bars* are two standard deviations. Note the young ages from high elevations, the small change in age over large elevation intervals and the lack of a "break in slope" as seen in Fig. 3. These younger ages at such high elevations reflect greater uplift and the exposure of deeper erosional levels.

Apatite ages older than 50 Ma and above ~1200 m a.s.l. in elevation define a shallow gradient (~15–50 m Ma^{-1}). Ages younger than 50 Ma and from elevations lower than 1200 m do not change significantly with elevation and define a much steeper gradient. A "break in slope" is evident in the apatite age–elevation pattern here at ~50 Ma and 1200-m elevation. A major implication of this two-component pattern in Fig. 3 is that this part of NVL and southern Victoria Land are extremely similar in their uplift histories. This group of apatite ages in Fig. 3, with the exception of the Helliwell Hills results, will be referred to hereafter as the "regional" pattern as it is typical of much of the area studied.

(2) Three samples from the Helliwell Hills all with apatite ages close to 100 Ma lie below the shallow gradient defined by the "regional" ages older than 50 Ma (Fig. 3).

(3) A single age from the Lichen Hills in the far western part of the study area of 304 ± 11 Ma was obtained from an elevation of 2085 m a.s.l. Because this was significantly different from any yet determined in the TAM, a second mount was prepared and dated. The result was indistinguishable from the first at 315 ± 10 Ma, confirming the measurement and giving a weighted mean age of 310 ± 7 Ma (Fig. 2). Subsequently, two further apatite ages were obtained from the Outback Nunataks at 196 ± 12 and 251 ± 17 Ma. These three ages from the most westerly areas sampled are all significantly older than any other apatite fission-track ages yet determined from Victoria Land. As such, they are unique in clearly pre-dating the Jurassic magmatic event responsible for intrusion of Ferrar Dolerite and eruption of Kirkpatrick Basalt.

(4) In the southeastern coastal region (the Mt. Murchison and Lower Tucker Glacier areas), apatite ages delineate a different pattern (Fig. 4). Here, the change in apatite age with elevation is small, and similar to that seen in the "regional" pattern for ages of <50 Ma. In the Mt. Northampton area in the Lower Tucker Glacier, the apatite ages vary little and range from 24 ± 2 to 34 ± 3 Ma over 2 km of elevation. Likewise, at Mt. Murchison, the ages vary from 26 ± 2 to 35 ± 4 Ma for the top four samples over 3.4 km of vertical section.

5.2. Track length measurements

Track length measurements were made on 26 apatite mounts. The results are summarised in Table III and presented graphically in Figs. 5 and 6. The uncertainty quoted for each mean length is given as the standard error of the mean, with the standard deviation giving a measure of the spread in each distribution. In the first instance, length distributions fall into two easily distinguishable groups (Table III). Apatite ages of <50 Ma have mean lengths generally of >14 μm with standard deviations of $< \pm 1.8$ μm. In contrast, ages older than 50 Ma have length distributions that are shorter and broader, with mean lengths usually between 12 and 13 μm and standard deviations $> \pm 2$ μm.

5.3. Zircon fission-track ages

Six samples were attempted but only three from the southeastern coastal region proved possible to date (Table II). Samples R*31714* and R*31717* from Mt. Murchison have apparent ages of 220 ± 16 and 250 ± 15 Ma, respectively. The lowermost sample from here has an age of 28 ± 2 Ma, similar to the apatite age. Note that the zircon ages here increase with increasing elevation. Sample R*31731* from Mt. Northampton in the Lower Tucker Glacier area has an age of 237 ± 33 Ma. Of these three samples, many grains from R*31717* and R*31731* were nearly metamict, in comparison to R*31714* which had a much greater percentage of good and countable grains. Zircon grains in the three samples attempted from the "regional" pattern (R*31702*, *-10* and *-33*) all appeared metamict after etching, indicating a significantly higher level of irradiation damage.

5.4. Sphene fission-track ages

All the eight sphene samples are from rocks mapped as the Admiralty Intrusives. Five of these results (Table II), incorporating all the "regional" ages and the top Mt. Murchison sample (R*31717*) in the southeastern coastal region cluster around a mean of 353 Ma. Spontaneous track densities were generally extremely high in these samples, approaching the limit for satisfactory counting. The other three samples from the coastal area are all significantly younger, especially R*31713* from the base of Mt. Murchison which has an age of 40 ± 3 Ma.

TABLE III

Analytical results - NVL confined fission-track lengths in apatite

Sample No.	Age (Ma)	Track length (±1σ) (μm)	Standard deviation (μm)	Number of tracks
"REGIONAL DATA"				
Ages less than 50 Ma: Morozumi Range, Aviator Glacier, Lillie-Ebbe Glacier, Yule Bay:				
R*31709*	44±4	13.60±0.18	1.79	101
R*31711*	37±2	14.25±0.14	1.38	100
R*31712*	44±2	14.44±0.15	1.48	100
R*31729*	48±7	14.01±0.12	1.21	99
R*31733*	42±2	14.14±0.18	1.85	111
Ages greater than 50 Ma: Admiralty Mountains, Freyberg Mountains:				
R*31705*	79±3	12.97±0.25	2.52	101
R*31706*	66±3	12.74±0.23	2.32	100
R*31707*	79±4	12.60±0.22	2.25	101
R*31708*	74±4	12.65±0.24	2.44	100
R*31718*	125±6	12.27±0.32	3.70	138
R*31719*	103±9	12.71±0.29	2.94	100
R*31720*	76±6	12.64±0.24	2.36	100
R*31723*	81±7	12.88±0.20	1.98	102
MT. MURCHISON				
R*31713*	27±3	14.59±0.17	1.66	96
R*31714*	26±2	14.68±0.11	1.15	100
R*31715*	29±2	14.49±0.16	1.51	84
R*31716*	36±4	14.54±0.18	1.21	47
R*31717*	30±2	14.49±0.16	1.63	100
LOWER TUCKER GLACIER				
R*31730*	34±2	14.20±0.15	1.54	102
R*31731*	24±2	13.99±0.15	1.36	87
R*31732*	34±3	14.34±0.16	1.60	100
HELLIWELL HILLS				
R*32173*	98±6	13.05±0.22	2.17	100
R*32204*	100±4	13.50±0.17	1.74	100
LICHEN HILLS-OUTBACK NUNATAKS				
R*31724*	310±7	12.25±0.16	1.57	100
R*31725*	196±12	13.18±0.22	2.18	100
R*31726*	251±17	11.96±0.22	2.20	101

6. Discussion and interpretation

6.1. Central and northern NVL

We have delineated a two-component uplift history for "regional" NVL similar to that seen in southern Victoria Land (Gleadow and Fitzgerald, 1987) and we can draw similar conclusions here in NVL as those in southern Victoria Land. The "break in slope" at ~50 Ma (Fig. 3) marks the base of an uplifted annealing zone

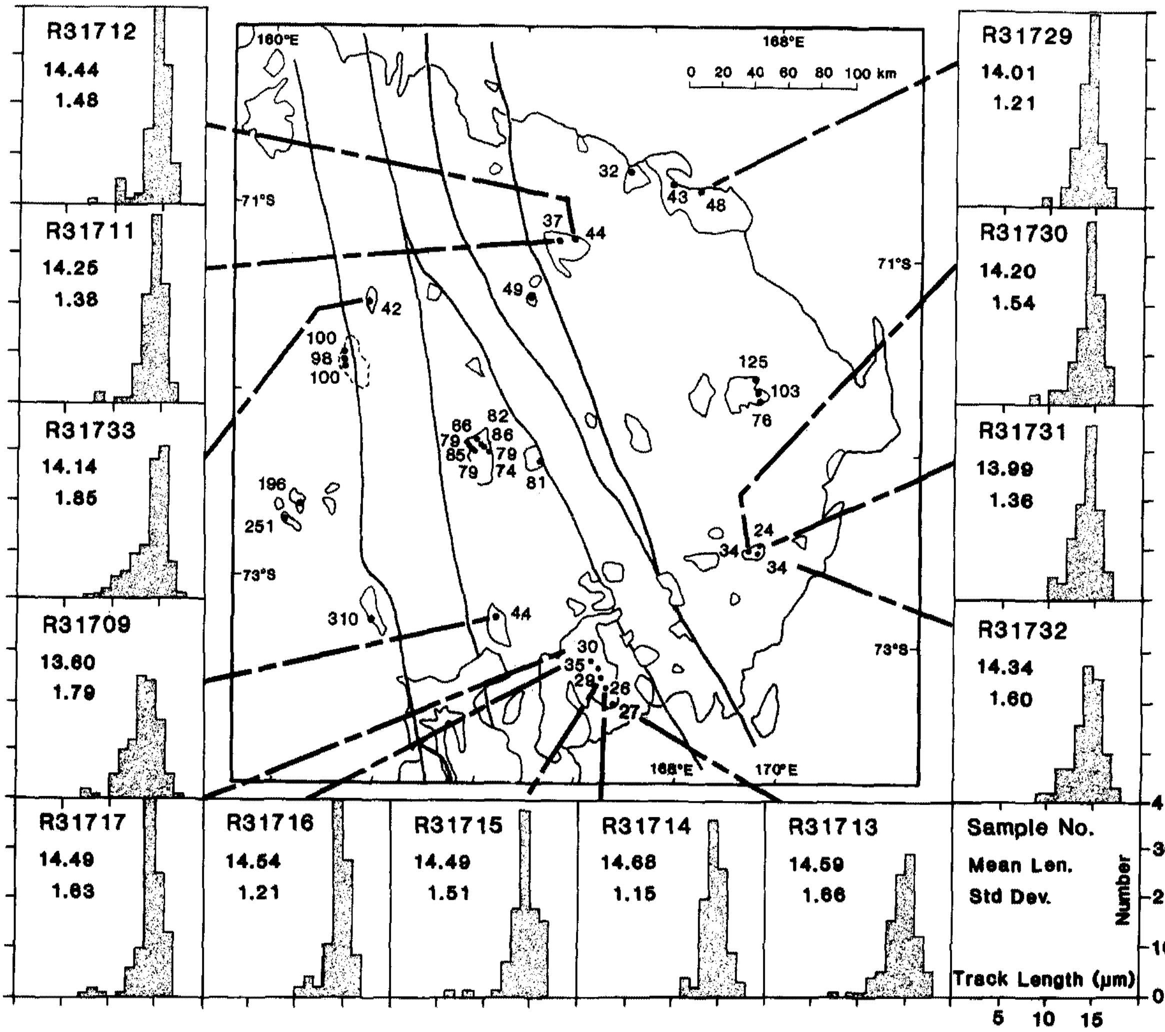

Fig. 5. Fission-track confined length distributions plotted according to location for samples of <50 Ma in age. Distributions are normalised to 100. All samples, except *R31709* have mean lengths of > 14 μm and standard deviations of < ± 1.85 μm.

and represents the time of initiation of uplift of the TAM. The shallow gradient defined by ages older than 50 Ma is an inherited characteristic from the pre-uplift apatite annealing zone. Ages younger than 50 Ma defining the steeper part of the apatite age profile are "uplift" ages, that is, they were recorded after uplift began. Prior to this, they lay below the base of the annealing zone at temperatures too high to record tracks.

Gleadow and Fitzgerald (1987) determined the amount of uplift at Mt. Doorly in southern Victoria Land by reconstructing the stratigraphic thickness above the "break in slope" seen in the apatite age profile. This is not possible in NVL however, because the stratigraphy is not as well ordered or as well known. Assuming that the thermal histories of NVL and southern Victoria Land were similar prior to uplift, we can use the calculated palaeo-geothermal gradient from southern Victoria Land to determine the depth to the base of the pre-uplift annealing zone (~100°C) in NVL. The

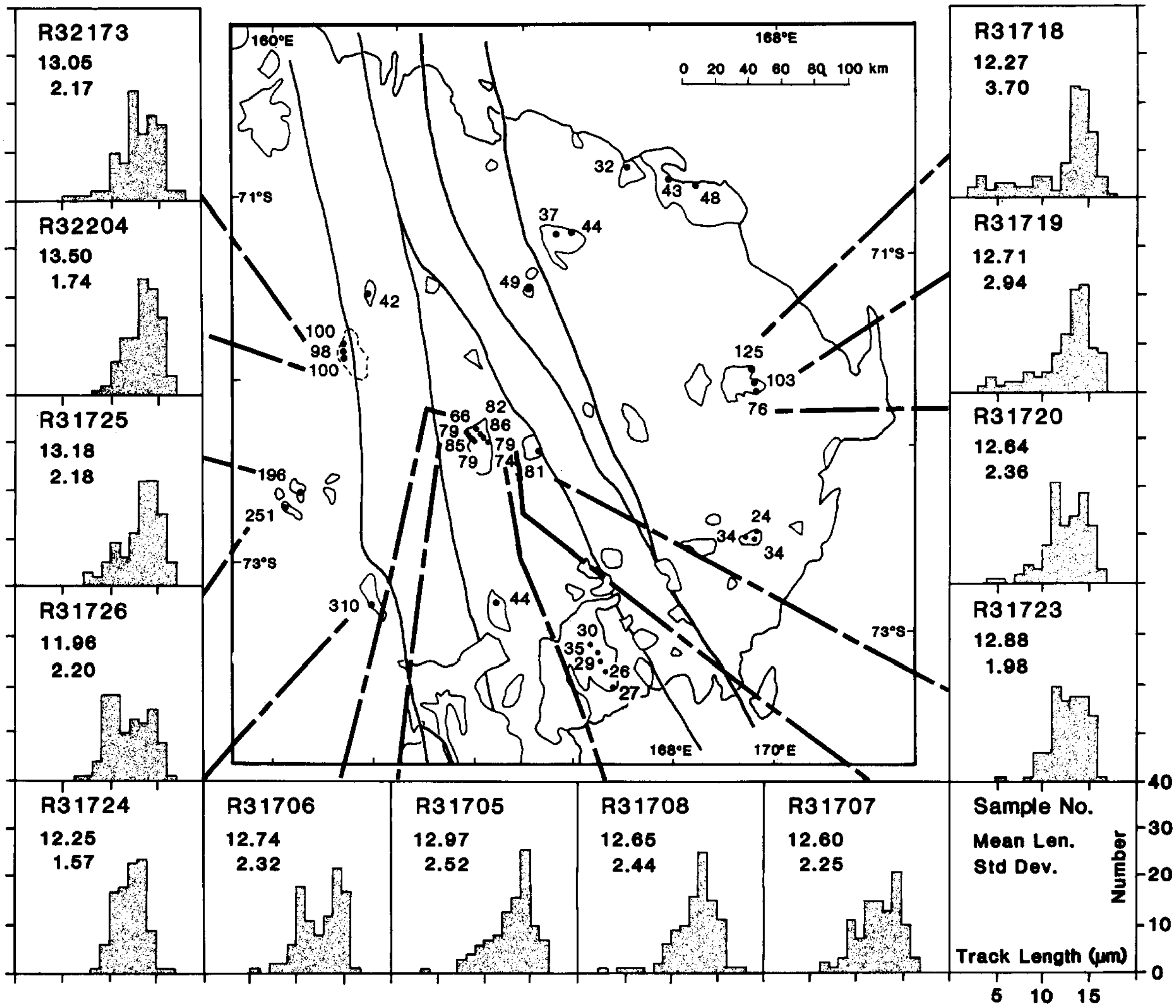

Fig. 6. Fission-track confined length distributions plotted according to location for samples > 50 Ma in age. Distributions are normalised to 100. Note the shorter mean lengths and much broader distributions compared to those in Fig. 5.

calculated pre-uplift (Late Cretaceous–early Cenozoic) geothermal gradient in southern Victoria Land was calculated to be ~25°C km^{-1}. Applying this method then, and using an assumed mean annual surface temperature of 0°C and a palaeo-surface elevation of between 0 and 500 m, the depth to the base of the annealing zone in NVL would have been ~3.5–4.0 km below sea-level. The "break in slope" for the "regional" ages is now at an elevation of ~1200 m above sea-level implying that there has been ~4.7–5.2 km of uplift since ~50 Ma.

Track length distributions for apatite samples below the "break in slope" from this region (Fig. 5), have long mean lengths (> 14 μm) and small standard deviations (1.15–1.85 μm) again closely paralleling the results from southern Victoria Land. This shows they have spent a relatively short time within the apatite annealing zone compared to time spent at lower temperatures (at a ratio of ~1:5). This indicates that the initial period of uplift was relatively rapid. An approximate uplift rate for the initial 10 Ma can be estimated from this 1:5 ratio to be ~200 m Ma^{-1}. If uplift had been continuous and at the average rate calculated over the full 50 Ma, then ~50% of the time elapsed since then would have been spent within the anneal-

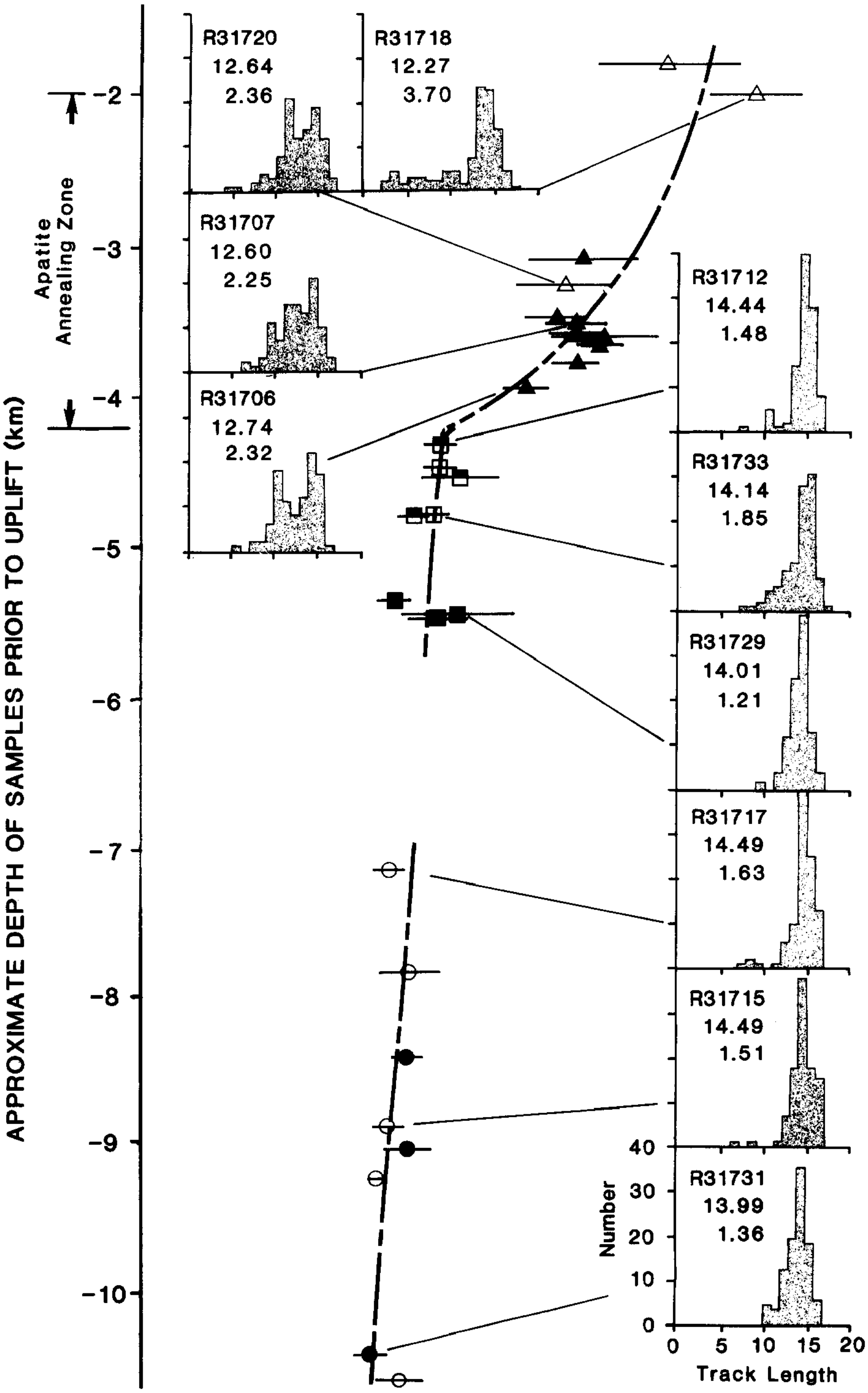

Fig. 7. Composite profile showing the relative positions of samples forming the "regional" pattern and those from the southeastern coastal area prior to uplift. It should not be interpreted to mean that the samples from the southeastern coastal area lay beneath the samples from the central and northern areas of NVL, nor on the same fault block. This diagram was drawn assuming the coastal samples have undergone an additional ~5 km of uplift. The distinct difference in track length distributions from samples above and below the base of the apatite annealing zone (the "break in slope") is clearly shown here. Samples below this point accumulated no tracks prior to uplift whereas samples above it have a component of shortened tracks from the annealing period prior to uplift and a later component of longer "uplift" tracks. This diagram has been constructed from the apatite age-elevation profiles (Figs. 3 and 4), but in a real pre-uplift situation the gradient for the line below the "break in slope" would be vertical because the apparent apatite ages then were zero.

ing zone and the length distributions would have means of ~ 13 μm with larger standard deviations.

Track length distributions for samples lying above the "break in slope" (Fig. 6) have significantly shorter mean lengths (~ 12.5 μm) and much larger standard deviations (> 2 μm). The difference in the length distributions for the two sections of the age–elevation profile can be clearly seen in Fig. 7 which shows reconstructed apatite age and track length data for samples in the relative positions they occupied prior to uplift. For the samples above the "break in slope" the tendency to bimodality in some of the length distributions and their consistently shorter, broader character indicates a much greater proportion of time spent within the annealing zone. These samples must also have experienced the same uplift since ~ 50 Ma as the relatively deeper samples so that this time spent within the annealing zone must have occurred prior to uplift. The survival of partially annealed tracks in these apatites is also reflected in their higher apparent ages (> 50 Ma). The differences in length distributions observed reflect the different levels occupied by the samples within the fossil annealing zone.

Samples R*31718* and R*31719* (Fig. 6) at the highest levels in the Admiralty Mountains do not have length distributions consistent with their reconstructed level (Fig. 7) in the pre-uplift apatite annealing zone. Their length distributions are too broad and too many short tracks are present compared to their inferred position at the very top of the Late Cretaceous–early Cenozoic annealing zone (Fig. 7). The significant proportion of short tracks in samples R*31718* and R*31719* could not have been produced in the time available at this inferred position if they had been completely overprinted in the Jurassic. Therefore, the significant number of short tracks is probably due to incomplete overprinting during the Jurassic thermal event accompanying Ferrar magmatism. The older ages in the western area show that the Jurassic thermal event did not raise temperatures high enough to erase fission tracks in apatites around the Lichen Hills and Outback Nunataks. Therefore these short tracks have probably survived from before Jurassic magmatism, at which time they underwent a high degree of track shortening. Sample R*31720* from nearby these other two samples (Fig. 1), but at a lower elevation, has a length distribution consistent with residence at its inferred position in the fossil annealing zone after complete overprinting in the Jurassic.

Therefore the isotherms during the Jurassic were raised enough to anneal the tracks in R*31720*, and reset it to zero, but not in R*31718* and R*31719* where tracks were only drastically shortened. These two samples are now at an elevation of 3.5 km and must have lain at a depth of ~ -1.5 km prior to uplift, assuming ~ 5 km of uplift since ~ 50 Ma. If the land-surface elevation at that time was between 0 and 500 m, then this constrains the amount of erosion above these samples to ~ 2 km. It should be remembered that these samples occur near the top of some of the highest peaks in the Admiralty Mountains and so this represents a minimum amount of erosion for the region.

6.2. Helliwell Hills

The Helliwell Hills samples plot ~ 1 km below the "regional" trend in Fig. 3. Because the shape of their track length distributions (Fig. 6) is similar to the "regional" samples a similar thermal history is envisaged. That they plot lower (Fig. 3) indicates less uplift of what is obviously a different fault block. Their slightly longer mean track lengths support this and indicate a relatively higher position within the fossil annealing zone. This is based on the assumption that uplift in all parts of NVL started ~ 50 Ma, a not unreasonable assumption in this case when it is considered that uplift in both the northern and central parts of NVL and southern Victoria Land was initiated at about the same time.

6.3. Lichen Hills–Outback Nunataks

The three ages from the Lichen Hills–Outback Nunataks all predate the Ferrar thermal event and as such they have escaped, at least partially, complete thermal overprinting at this time. The track length distributions appear to follow the age trend (Fig. 6). Sample R*31724* from the Lichen Hills with an age of 310 ± 7 Ma has the narrowest spread of the three, sample R*31726* from the Outback Nunataks, the next oldest at 251 ± 17 Ma has almost a bimodal distribution and R*31725*, at 196 ± 12 Ma has a much reduced shorter track component.

Stump et al. (1986) in their reconstruction of Australia and Antarctica, correlate the Delamerian terrane of southeastern Australia with the Wilson terrane of NVL. Apatite fission-track ages from granitic rocks in the Dundas Tableland, on the eastern side of the Delamerian terrane, range from 316 ± 14 to 384 ± 10 Ma and are interpreted as slow cooling ages following Ordovician–Devonian emplacement (Gleadow and Lovering, 1978). In contrast to NVL, the Delamerian terrane was not affected by major Jurassic magmatism, although some volcanics of this age are known, nor has it undergone significant Cenozoic uplift. As such these apatite ages are similar to the single apatite age from the Lichen Hills which lies within the southern extension of the Wilson terrane. A similar thermal history relatively undisturbed by post-Palaeozoic events is therefore envisioned for this sample, although its slightly younger age probably reflects very slight overprinting during Jurassic magmatism. The relative proportion of short tracks to long tracks indicates that it has not resided near the base of the annealing zone but rather closer to the top, for most of its history before being uplifted.

It may seem strange that R*31726* which has an older apatite age (251 ± 17 Ma) than R*31725* (196 ± 12 Ma) has a shorter mean length. This can again be explained by the thermal effect of the Jurassic dolerites and the relative proportion of short to long tracks. R*31725* was more affected than R*31726*, as can be seen by a greater age reduction, but because of this it has a smaller short track component. In other words, there are only ~16 Ma of tracks left in R*31725* from before the Jurassic magmatism, and these will be short because the sample has almost been completely overprinted, reducing the age from ~310 Ma or more, to 196 Ma. This compares to ~70 Ma of "pre-Jurassic" tracks present in R*31726*, which has not undergone the same amount of annealing but retains a greater overall proportion of short tracks because of it. Hence the relative number of short tracks in R*31726* is greater, resulting in a decrease in the overall mean track length of this sample.

The Outback Nunatak samples with younger ages and broader track length distributions suggest a degree of partial annealing compared to the sample from the Lichen Hills (Fig. 6). Their higher elevations than the Lichen Hills sample suggests that a lower position within the pre-uplift annealing zone was not responsible for this modification. Therefore, partial overprinting during the Jurassic is more likely to be responsible for the reduced ages and spread in the length distribution. Preservation of older ages in these western areas suggests that less erosion has occurred relative to that observed further east. It is likely that because the Lichen Hills–Outback Nunataks are to the west of the Rennick Graben in a similar position to the Helliwell Hills, on a fault block on a similar level, that both these areas underwent the same amount of uplift.

6.3. Southeastern coastal region

In the southeastern coastal region, there is no "break in slope" in the apatite age–sample elevation profile (Fig. 4), but the ages and track length distributions are similar to those for the "regional" ages of < 50 Ma. A similar thermal history is therefore envisaged. The presence of these younger apatite ages at much higher elevations than in the "regional" area implies much more uplift and erosion and the exposure of deeper crustal levels. If we assume that uplift began at the same time for these adjacent areas (~50 Ma) as in the rest of NVL, it is possible to crudely estimate the amount of uplift by extrapolating the "apparent uplift gradient" upwards until it intersects 50 Ma. Extrapolation of this line intersects 50 Ma at an elevation of ~6000 ± 2000 m. Unfortunately the data set is neither large enough nor well enough constrained to say more than that uplift here has been in the order of 5 (± ~2) km, more than that calculated for the central and northern parts of NVL.

In Fig. 7 we have reconstructed apatite age and track length data for samples in the relative positions they are inferred to have occupied prior to uplift. This diagram shows the variation of track length distributions for samples above and below the "break in slope" as well as the observation that the apatite fission-track data from these two areas form a continuum which is best interpreted in terms of differential uplift. When viewing this diagram it is important to appreciate the fact that these two areas have differing uplift histories and this is an attempt to portray the relative depths at which the samples formerly resided, and hence the relative amount of uplift they have undergone. It does not imply they lie on the same fault block, but rather, that the samples from the southeastern coastal area lay relatively lower in the crust than samples from central and northern NVL prior to uplift.

6.4. Zircon and sphene ages

Fission tracks in zircons and sphenes anneal at higher temperatures than fission tracks in apatite. Extrapolation of annealing experiments suggests closure temperatures in excess of 300°C for zircon (Fleischer et al., 1965; Krishnaswami et al., 1974) whilst geological arguments have suggested a lower temperature of 175–250°C (e.g., Harrison et al., 1979; Zeitler et al., 1982). Gleadow and Brooks (1979) used a temperature of 200 ± 50°C, Zeitler (1985) determined a closure temperature of 250°C, and recently, Hurford (1986) calculated a closure-temperature of 240 ± 50°C for the effective track retention temperature in zircon. Sphene ages are usually concordant or older than zircon fission-track ages in slowly cooled terrains, and sphene ages are often comparable to K–Ar biotite ages. Gleadow and Brooks (1979) used a closure temperature of 250 ± 50°C for sphene and Harrison et al. (1979) argued that the sphene annealing zone was no different to the epidote annealing zone which they estimated as 200–280°C. Based on the limited available evidence, we infer ~250°C for the base of the zircon annealing zone and 300°C for the base of the sphene annealing zone.

The three zircon ages from Mt. Murchison progressively decrease in age with decreasing elevation, from an age of 250 ± 15 Ma near the summit to 28 ± 2 Ma at the base of the mountain (Table II). All these samples have ages that are reduced compared to the emplacement age of the Admiralty Intrusives. The lowermost sample (R*31713*) near sea-level, with an age of 28 ± 2 Ma is comparable to the apatite age from here and it passes the χ^2-test, indicating little real variation in single grain ages. This suggests that it, like the apatite age from this locality, has been totally overprinted prior to major Cenozoic uplift. The next oldest age from Mt. Murchison (R*31714*), 220 ± 16 Ma at 1345-m elevation fails the χ^2-test, as does the zircon age of 237 ± 33 Ma from 175 m on Mt. Northampton (R*31731*), which suggests some element of annealing is responsible for the age reduction. The summit sample from Mt. Murchison (R*31717*, 250 ± 15 Ma) probably represents a slow cooling age since the time of emplacement of the Admiralty Intrusives or only partial annealing. This suggests that an uplifted zircon annealing zone is revealed between the bottom and top of Mt. Murchison.

Sphene ages of 344 ± 15 to 372 ± 15 Ma from the central and northern part of NVL (Table II; Fig. 2) are comparable, although less precise, to K–Ar biotite ages of 358–366 Ma

(Kreuzer et al., 1981) for the high-level Admiralty Intrusives. The uppermost sample at Mt. Murchison (R*31717*) has a similar sphene age to this grouping, reflecting initial cooling after emplacement in the Late Devonian. However, the lowermost sample from Mt. Murchison (R*31713*) has a different age (40 ± 3 Ma), broadly comparable to both the zircon and apatite age for this sample, again suggesting total overprinting prior to major Cenozoic uplift. This suggests that between the lowermost sample at Mt. Murchison and the summit sample, an entire uplifted sphene annealing zone is revealed. Sphenes from Mt. Northampton also show some reduction in age, suggesting they too are annealed. Using the assumed pre-uplift geothermal gradient of $\sim 25°$C, the depth to the base of both the zircon and sphene annealing zones is consistent with uplift in the vicinity of 10 km.

Another possibility may exist to explain the almost concordant apatite, zircon and sphene ages for the lowermost Mt. Murchison sample (R*31713*). They may in fact come from a Tertiary intrusive. Stump et al. (1983) found a Tertiary granite in the lower Mariner Glacier, dating it at 9 ± 1 Ma. They described it as a medium-graded granite composed of a secondary assemblage of quartz, K-feldspar, albite and chlorite. The original assemblage was probably two feldspars and quartz with numerous miarolitic cavities, suggesting a shallow level of emplacement. They went on to add that the McMurdo volcanics may have provided heat for generation of this granite melt but that the source region for this silicic magma was undoubtedly lower crustal compared to a mantle source for the mafic magmas of the McMurdo Volcanics. Sample R*31713* is a medium-grained very hornblende-rich quartz diorite of I-type affinity. This sample came from a granitic body that occurred dominantly as veins containing $\sim 50\%$ of country rock xenoliths. This compares to the usual massive appearance of the granites of the Admiralty Intrusives. However, given that the apatite age from this locality appears to belong to a more regional trend and the rock type is similar to the typical Admiralty granite, it is considered that it is unlikely to be a Tertiary granite.

6.5. Summary of thermal histories

The apatite results from the central and northern parts of NVL (the "regional" pattern) are remarkably similar to the results from southern Victoria Land and a similar thermal history is envisaged. Samples above the "break in slope" lay at varying levels in a pre-uplift apatite annealing zone and samples below the "break in slope" had a zero apparent age prior to uplift. The shapes of the track length distributions confirm this interpretation and provide additional information. Track length distributions for samples below the "break in slope" indicate that these samples have spent little time within the apatite annealing zone and hence initial uplift over about the first 10 Ma must have been rapid. Track length distributions from samples R*31718* and R*31719* in the Admiralty Mountains are not consistent with their reconstructed level in the pre-uplift annealing zone, suggesting these two samples were only partially overprinted during the Jurassic. This contrasts with all other samples in the regional pattern (central and northern areas of NVL) which were effectively reset to zero at that time. Isotherms in the Admiralty Mountains must have been elevated enough to erase all tracks in R*31720* (at a lower elevation) but only partially erase and shorten tracks in R*31718* and R*31719* (at higher elevations).

The ages from the Helliwell Hills plot lower than the regional pattern, yet their track length distributions are similar indicating a similar sort of thermal history although their slightly longer length indicates that the Helliwell Hills samples resided at a higher level than most of the regional samples. This is consistent with less uplift (1–2 km) for these samples. Out to the west in the Lichen Hills and Outback Nunataks the old ages show that the Jurassic thermal event associated with the intrusion of dolerite and extrusion of flood basalts did not completely reset these samples, although they have been partially annealed and show progressive degrees of this.

The variety of thermal histories present in NVL can be traced in a plot of apatite age against mean track length (Fig. 8). The extreme right of the diagram is where the original slow cooling ages of the granites plot. Ages then decrease to the left with increasing amounts of annealing due to Jurassic magmatism. Mean track lengths here initially decrease and then increase owing to the relative proportions of short partially annealed pre-Jurassic tracks and relatively long post-Jurassic tracks.

Nearly all ages younger than 180 Ma were completely reset by Jurassic magmatism, the two exceptions being samples R*31718* and R*31719* from the Admiralty Mountains (Fig. 8), which were only partially overprinted and then resided in the subsequent annealing zone. Three different components of track length make up the length distribution for these two samples accounting for their exceptionally large standard deviations. They have a set of pre-Jurassic tracks drastically shortened by the thermal event accompanying magmatism, they have a set of relatively short tracks from residence

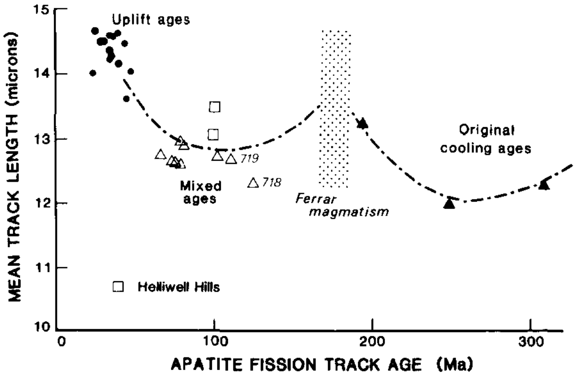

Fig. 8. Apatite fission-track age plotted against mean track length. *Solid dots* represent ages of < 50 Ma, *open triangles* ages of > 50 Ma, and *solid triangles* are the three samples from the Lichen Hills-Outback Nunataks that have escaped complete overprinting by the Ferrar thermal event. This plot can be used to summarize the thermal histories existing in NVL. See text for explanation.

within the pre-uplift apatite annealing zone and they have a set of long tracks recorded after major uplift in the early Cenozoic. Other samples with ages between 180 and 50 Ma were reset to zero in the Jurassic and have only the later two components making up their track length distributions which have mean lengths of 12–13 μm and standard deviations reflecting a two-stage history. Samples with ages younger than 50 Ma with long lengths generally greater than 14 μm and small standard deviations indicate a simple thermal history accompanying an initial period of rapid uplift.

6.6. *Tectonic implications*

Different amounts of uplift have been proposed for different areas of NVL and these are summarised in Fig. 9. As described above, the pre-Palaeozoic geology of NVL is controlled by a number of major NW–SE-trending faults and it is apparent that block faulting controls the post Beacon/Ferrar deformation. In describing the uplift of central and northern NVL (the "regional" pattern) so far, we have tended to refer to it as a single entity. This is obviously an oversimplification because varying angles of dip of the sub-Beacon erosion surface on blocks in the order of 10 km across (Walker, 1983), imply differential movement between different fault blocks. Slight tilting between these blocks is probably present throughout the central and northern area but is not enough to be evident in the apatite fission-track data.

It is evident from the fission-track results that in the western part of NVL there has been ~1 km less uplift than for the central and northern parts. These two regions are separated by the Rennick Glacier which is believed to be a complex graben (Fig. 9) (Gair et al., 1969). The Rennick Fault which bisects the Helliwell Hills with a downthrow of 600 m on its eastern side defines the western boundary of the Rennick Graben (Sturm and Carryer, 1969). Dow and Neall (1974) located a further fault on the east side of the Morozumi Range with a downthrow

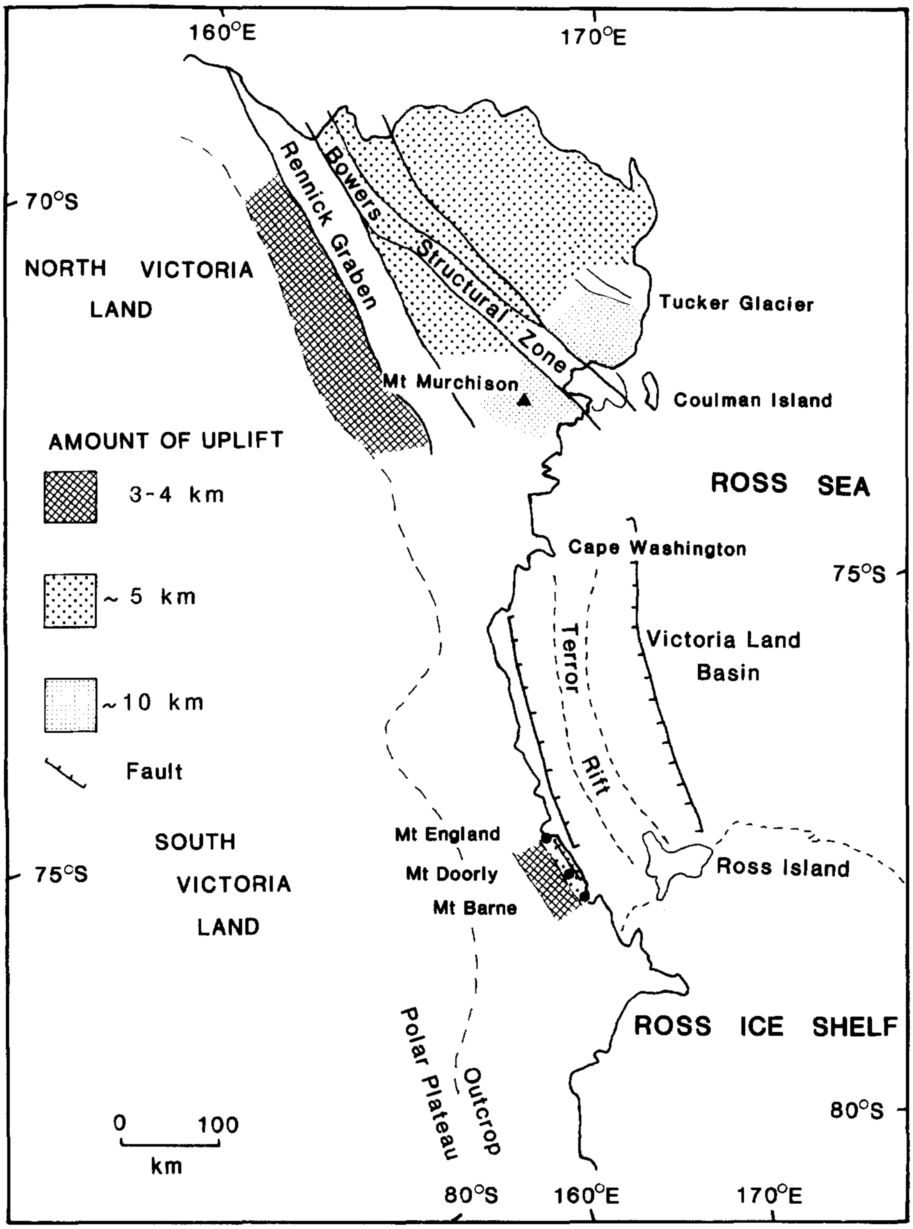

Fig. 9. Map of the entire Victoria Land region showing the relative positions of the Victoria Land Basin, Rennick Graben and Bowers Structural Zone. Tectonic boundaries for NVL from Fig. 1 and from A.K. Cooper and Davey (1985) and A.K. Cooper et al. (1987) for the Victoria Land Basin. The amount of uplift in NVL determined by this study is also shown. In southern Victoria Land, the amount of uplift is also shown as are three localities where this has been determined. These are Mt. England (P.G. Fitzgerald, unpublished data, 1987), Mt. Doorly (Gleadow and Fitzgerald, 1987) and Mt. Barnes (Fitzgerald, 1986). Inland of these localities the amount of uplift decreases westwards and is defined by the dip of the Kukri peneplain (2-3°), whereas on the seaward side a number of listric normal faults exist stepping down to the coast and towards the western boundary of the Victoria Land Basin (Fitzgerald et al., 1986).

of 300 m to the east. Therefore parts of the Rennick Graben are downthrown at least 1.9 km relative to its eastern flank and at least 0.9 km relative to its western flank. This compares to a depth of 2 km for the Rennick Graben determined by T. Stern (pers. commun., in Grindley and Oliver, 1983).

In the western part of NVL, strata of the Beacon Supergroup dip gently to the west under the polar icecap at ~2–3°. The amount of uplift probably decreases westerly at this same rate, similar to the pattern observed on the western side of the TAM in southern Victoria Land (Gleadow and Fitzgerald, 1987). Lying ~50–100 km to the west of NVL is the Wilkes Subglacial Basin which reaches depths of 1300 m below sea-level (Drewry, 1983). It is not known whether the TAM gently descend to the eastern edge of this basin or whether the boundary is fault controlled, but it is unlikely that faults of the magnitude seen in places on the coastal margin of the TAM exist on this side of the range.

Differential amounts of uplift on fault-controlled blocks as suggested here, and the Rennick Faulting as defined by Tessensohn et al. (1981) are most likely the same event, and a result of the uplift and formation of the TAM. The apatite age of 42±2 Ma from an elevation of 700 m in the Morozumi Range lying within the confines of the Rennick Graben, suggests the timing of this faulting may be early Cenozoic. However, because of the small variation in apatite age over significant elevation changes with respect to uncertainties for apatite ages of <50 Ma, this particular result cannot be used as a tectonic marker.

Fitzgerald et al. (1986) have recently related the uplift and formation of the TAM to extension and subsidence leading to the formation of sedimentary basins within the Ross Embayment. If the Rennick Faulting is related to the uplift and formation of the TAM in NVL then the formation of the Rennick Graben is also related to the formation of sedimentary basins in the Ross Embayment. A.K. Cooper et al. (1987) have suggested that the Victoria Land Basin, in particular the Terror Rift (Fig. 9) is an en echelon structure along a north–south rift zone. They add that if the Rennick Graben and Victoria Land Basin were continuous features, then the intervening granitic basement was either uplifted or was high standing prior to rifting. If this rift, or zone of extension was continuous during the late Mesozoic–early Cenozoic, then it is possible, indeed likely that an intervening basement block was uplifted, as the position of this postulated block lies just south of the Mt. Murchison region where we have estimated uplift in the order of 10 km.

Fitzgerald et al. (1986) suggested that uplift of the TAM and subsidence in the Ross Embayment was a result of differential partition of strain into a crustal level in the Ross Embayment and into the mantle lithosphere under the TAM. Two periods of extension seem to be resolvable within the Ross Embayment (A.K. Cooper et al., 1987). The first (Late Cretaceous to early Cenozoic) appears to have affected all three basins and may be responsible for their formation, whilst the second (possibly Oligocene to recent) has affected only the Victoria Land Basin. It is possible that the eastern bulge of NVL may have complicated the pattern of extension in the Ross Sea, in particular with regard to the area immediately north of the Victoria Land Basin. The eastern bulge of NVL (composed mainly of the Robertson Bay terrane) may have caused the axis of extension in the Victoria Land Basin to bifurcate just south of Cape Washington, resulting in the formation of the Rennick Graben which later became cut off, and a crustal extension zone running from Cape Washington to Cape Hallett, as marked now by the Cenozoic volcanics along the coast (Fig. 1).

The proposed northwesterly extensional trend up the Rennick Graben follows an inherent line of weakness coinciding with the outcrop pattern of the Jurassic magmatism in NVL (Fig. 1). It is possible that if extensional zones existed either side of the southeastern coastal region of NVL, where there is an estimated 10 km of uplift, that this could explain the much greater uplift seen in the Mt. Murchison and Lower Tucker Glacier areas which lie just north of Cape Washington (Fig. 9). By implication, this means that the mantle lithosphere under this uplifted area was even more thinned than in other places under the TAM, hence giving a greater isostatic response. Little is known about the crustal structure under NVL, or under the Robertson Bay terrane and it is possible that in places the Robertson Bay terrane may have a thicker crust than elsewhere under the TAM, or this area may be thickened due to underplating, in either case isostatic uplift caused by lithospheric thinning would be enhanced.

7. Conclusions

A variety of thermal histories can be ascertained from the fission-track results in different parts of NVL and these combine to reveal the uplift history of the TAM in this area. As is the case in southern Victoria Land, the apatite age profiles reveal an age of ~50 Ma for the onset of uplift of the TAM in NVL. In the central and northern area of NVL the base of an uplifted apatite annealing zone is revealed and from this ~5 km of uplift is estimated. In the western part of the study area uplift is estimated to be 1–2 km less. In the southeastern coastal area, apatite results are interpreted to indicate uplift in the order of 10 km. The effect of the Jurassic thermal perturbation may be loosely constrained to an approximately north–south-trending zone between the Lichen Hills–Outback Nunataks region and the Mt. Royalist–Mt. Ajax area of the Admiralty Mountains, corresponding to its known extent in outcrop. In the Mt. Murchison area there is evidence of uplifted sphene and zircon annealing zones which is consistent with uplift in the order of 10 km as suggested by the apatite results.

For the central and northern parts of NVL the timing of uplift is relatively well constrained, as is the amount of uplift. The initiation time of uplift for the rest of NVL is assumed to be synchronous with this. An average uplift rate determined over this time period is essentially meaningless as variable rates of uplift exist. Track length distributions indicate a period of relatively rapid uplift during the initial stages of uplift. This can be very approximately estimated from the slope of the apatite age profile for ages of $< \sim 50$ Ma and from the shape of the track length distributions at ~ 200 m Ma^{-1} for the central and northern parts ("regional" pattern) and close to 400 m Ma^{-1} for the southeastern coastal area.

Structurally, the uplift to form the TAM is probably characterised by a mosaic of differentially tilted blocks as defined by varying dips and dip directions of the sub-Beacon erosion surface in different localities. Rennick Faulting seems undoubtedly related to the uplift and formation of the TAM in NVL and is probably related, at least temporally, to the formation of the Victoria Land Basin.

Acknowledgements

We wish to thank Ed Stump and John Holloway for the invitation to join their event during the 1981/1982 International North Victoria Land Expedition. The pilots and crew of VXE-6 working out of NVL base camp are warmly acknowledged for their assistance during sample collection. The Australian and New Zealand Antarctic Divisions are thanked for support and supply of field equipment to A.J.W.G. The Australian Research Grants Scheme provided financial assistance and the Australian Institute of Nuclear Science and Engineering paid for irradiation costs. P.G.F. was supported by a Melbourne University Postgraduate Scholarship. Mike Sandiford is thanked for willingly providing us with samples from the Helliwell Hills. Paul Green kindly counted two of the zircon mounts. We thank various members of the Melbourne University Fission Track Research Group for their contributions, especially Paul Green and Peter Kamp for comments on this manuscript and Glenn Duddy for his flawless sample preparations. This project forms part of the Melbourne University Programme in Antarctic Studies.

References

Adams, C.J.D., Gabites, J.E., Wodzicki, A., Laird, M.G. and Bradshaw, J.D., 1982. Potassium-argon geochronology of the Precambrian-Cambrian Wilson and Robertson Bay Groups and Bowers Supergroup, north Victoria Land, Antarctica. In: C. Craddock (Editor), Antarctic Geoscience. University of Wisconsin Press, Madison, Wisc., pp. 543-548.

Barrett, P.J., Grindley, G.W. and Webb, P.N., 1972. The Beacon Supergroup of East Antarctica. In: R.J. Adie (Editor), Antarctic Geology and Geophysics. Universitetforslaget, Oslo, pp. 319-332.

Bradshaw, J.D. and Laird, M.G., 1983. Pre-Beacon geology of northern Victoria Land: a review. In: R.L. Oliver, P.R. James and J.B. Jago (Editors), Antarctic Earth Science. Australian Academy of Science, Canberra, A.C.T., pp. 98-101.

Bradshaw, J.D., Laird, M.G. and Wodzicki, A., 1982. Structural style and tectonic history in northern Victoria Land. In: C. Craddock (Editor), Antarctic Geoscience. University of Wisconsin Press, Madison, Wisc., pp. 809-816.

Bradshaw, J.D., Weaver, S.D. and Laird, M.G., 1985. Suspect terranes and Cambrian tectonics in northern Victoria Land, Antarctica. In: D.G. Howell (Editor), Tectonostratigraphic Terranes of the Circum-Pacific Region. Circ.-Pac. Counc. Energy Miner. Resour., Earth Sci. Ser. No. 1, Houston, Texas, pp. 467-479.

Brady, H. and McKelvey, B.C., 1979. Some aspects of the Cenozoic glaciation of south Victoria Land, Antarctica. J. Glaciol., 29: 343-349.

Bryant, B. and Naeser, C.W., 1980. The significance of fission-track ages of apatite in relation to the tectonic history of the Front and Sawatch Ranges, Colorado. Geol. Soc. Am. Bull., 91: 156-164.

Calk, L.C. and Naeser, C.W., 1973. The thermal effect of a basalt intrusion on fission tracks in quartz monzonite. J. Geol., 81: 189-198.

Chappell, B.W. and White, A.J.R., 1974. Two contrasting granite types. Pac. Geol., 8: 173-174.

Cooper, A.K. and Davey, F.J., 1985. Episodic rifting of Phanerozoic rocks in the Victoria Land Basin, western Ross Sea, Antarctica. Science, 229: 1085-1087.

Cooper, A.K., Davey, F.J. and Behrendt, J.C., 1987. Seismic stratigraphy and structure of the Victoria Land Basin, western Ross Sea, Antarctica. In: A.K. Cooper and F.J. Davey (Editors), The Antarctic Continental Margin: Geology and Geophysics of the Western Ross Sea. Am. Assoc. Pet. Geol., Houston, Texas, Earth Sci. Ser., 5B: 27-76.

Cooper, R.A., Jago, J.B., Rowell, A.J. and Braddock, P., 1983. Age and correlation of the Cambrian-Ordovician Bowers Supergroup, northern Victoria Land. In: R.L. Oliver, P.R. James and J.B. Jago (Editors), Antarctic Earth Science. Australian Academy of Science, Canberra, A.C.T., pp. 128-131.

Crowley, K.D., Ahern, J.L. and Naeser, C.W., 1985. Origin and epeirogenic history of the Williston Basin: evidence from fission-track analysis of apatite. Geology, 13: 620-623.

Dalziel, I.W.D. and Elliot, D.H., 1983. The Antarctic plate: a global perspective. Penrose Conf. Rep., Geology, 11: 118-120.

Denton, G.H., 1979. Glacial history of the Byrd-Darwin Glacier area, Transantarctic Mountains. Antarct. J. U.S., 14: 57-58.

Dodge, F.C.W. and Naeser, C.W., 1968. Ages of apatites from granitic rocks of the Sierra Nevada Batholith. Trans. Am. Geophys. Union, 49: 348 (abstract).

Dodson, M.H., 1973. Closure temperature in cooling geochronological and petrological systems. Contrib. Mineral. Petrol., 40: 259-274.

Dow, J.A.S. and Neall, V.E., 1974. Geology of the Lower Rennick Glacier, northern Victoria Land. N.Z. J. Geol. Geophys., 17: 659-714.

Drewry, D.J. (Editor), 1983. Antarctic Glaciological and Geophysical Folio. Scott Polar Res. Inst., University of Cambridge, Cambridge.

Fershtater, G.B., Chashchukhina, V.A. and Vilisov, V.A., 1984. Fluorine and chlorine distribution in apatite occluded in different minerals of igneous rocks. Translated from: Respredeleniye flora i khlora v apatite, vklyuchennom v raznyye poradoobrazuyushchiye mineraly magmaticheskikh porod. Dokl. Akad. Nauk S.S.S.R., 276: 1228-1234.

Fitzgerald, P.G., 1986. Fission track studies of the Transantarctic Mountains, Beardmore Glacier area. Antarct. J. U.S. (in press).

Fitzgerald, P.G., Sandiford, M., Barrett, P.J. and Gleadow, A.J.W., 1986. Asymmetric extension associated with uplift and subsidence of the Transantarctic Mountains and Ross Embayment. Earth Planet. Sci. Lett., 81: 67-78.

Fleischer, R.L., Price, P.B. and Walker, R.M., 1965. Effects of temperature, pressure and ionization on the formation and stability of fission tracks in minerals and glasses. J. Geophys. Res., 70: 1497-1502.

Gair, H.S., 1967. The geology from the upper Rennick Glacier to the coast, northern Victoria Land, Antarctica. N.Z. J. Geol. Geophys., 10: 309-344.

Gair, H.S., Sturm, A., Carryer, S.J. and Grindley, G.W., 1969. The Geology of northern Victoria Land (Sheet 13). In: V.C. Bushnell and C. Craddock (Editors), Geologic Maps of Antarctica 1:1,000,000, Antarct. Map Folio Ser., Folio 12 P1 XII.

Gibson, G.M., 1985. Lanterman Fault: boundary between allochtonous terranes, northern Victoria Land, Antarctica. In: E. Leitch (Editor), Geol. Soc. Aust., Vol. 14 Abstracts, 3rd Circ-Pac. Terrane Conf., Sydney, N.S.W., pp. 79-82.

Gibson, G.M. and Wright, T.O., 1985. Importance of thrust faulting in the tectonic development of northern Victoria Land, Antarctica. Nature (London), 315: 480-483.
Gleadow, A.J.W., 1981. Fission track dating methods: what are the real alternatives? Nucl. Tracks, 5: 3-14.
Gleadow, A.J.W. and Brooks, C.K., 1979. Fission track dating, thermal histories and tectonics of igneous intrusions in East Greenland. Contrib. Mineral. Petrol., 71: 45-60.
Gleadow, A.J.W. and Duddy, I.R., 1981. A natural long term annealing experiment for apatite. Nucl. Tracks, 5: 169-174.
Gleadow, A.J.W. and Fitzgerald, P.G., 1987. Uplift history and structure of the Transantarctic Mountains: new evidence from fission track dating of basement apatites in the Dry Valleys area, southern Victoria Land. Earth Planet. Sci. Lett., 82: 1-14.
Gleadow, A.J.W. and Lovering, J.F., 1978. Thermal history of granitic rocks from western Victoria: a fission-track dating study. J. Geol. Soc. Aust., 25: 323-340.
Gleadow, A.J.W., Hurford, A.J. and Quaife, R.D., 1976. Fission track dating of zircon: improved etching techniques. Earth Planet. Sci. Lett., 33: 273-276.
Gleadow, A.J.W., Duddy, I.R. and Lovering, J.F., 1983. Fission track analysis: a new tool for the evaluation of thermal histories and hydrocarbon potential. Petrol. Explor. Assoc. Aust. J., 23: 9-102.
Gleadow, A.J.W., McKelvey, B.C. and Ferguson, K.U., 1984. Uplift history of the Transantarctic Mountains in the Dry Valleys area, southern Victoria Land, Antarctica, from apatite fission track ages. N.Z. J. Geol. Geophys., 27: 457-464.
Gleadow, A.J.W., Duddy, I.R., Green, P.F. and Hegarty, K.A., 1986a. Fission track lengths in the apatite annealing zone and the interpretation of mixed ages. Earth Planet. Sci. Lett., 78: 245-254.
Gleadow, A.J.W., Duddy, I.R., Green, P.F. and Lovering, J.F., 1986b. Confined fission track lengths in apatite - a diagnostic tool for thermal history analysis. Contrib. Mineral. Petrol., 94: 405-415.
Green, P.F., 1981. A new look at statistics in fission track dating. Nucl. Tracks, 5: 77-86.
Green, P.F., 1985. Comparison of zeta calibration baselines for fission-track dating of apatite, zircon and sphene. Chem. Geol. (Isot. Geosci. Sect.), 58: 1-22.
Green, P.F., Duddy, I.R., Gleadow, A.J.W., Tingate, P.T. and Laslett, G.M., 1985. Fission-track annealing in apatite: track length measurements and the form of the Arrhenius plot. Nucl. Tracks, 10: 323-328.
Green, P.F., Duddy, I.R., Gleadow, A.J.W., Tingate, P.R. and Laslett, G.M., 1986. Thermal annealing of fission tracks in apatite, 1. A qualitative description. Chem. Geol. (Isot. Geosci. Sect.), 59: 237-253.
Green, P.F., Duddy, I.R., Gleadow, A.J.W. and Lovering, J.F., 1988. Apatite fission track analysis as a paleotemperature indicator for hydrocarbon exploration. In: N.D. Naeser and T.H. McCulloh (Editors), Thermal Histories of Sedimentary Basins - Methods and Case Histories. Springer, Berlin (in press).
Grindley, G.W. and Oliver, P.J., 1983. Post-Ross Orogeny cratonisation of northern Victoria Land. In: R.L. Oliver, P.R. James and J.B. Jago (Editors), Antarctic Earth Science. Australian Academy of Science, Canberra, A.C.T., pp. 133-139.
Gunn, B.M. and Warren, G., 1962. Geology of Victoria Land between the Mawson and Mulock Glaciers, Antarctica. Bull. N.Z. Geol. Surv., No. 71, 157 pp.
Haack, U., 1977. The closing temperature for fission track retention in minerals. Am. J. Sci., 277: 459-464.
Harrison, T.M., Armstrong, R.L., Naeser, C.W. and Harakal, J.E., 1979. Geochronology and thermal history of the Coast Plutonic complex, near Prince Rupert, B.C. Can. J. Earth Sci., 16: 400-410.
Hurford, A.J., 1986. Cooling and uplift patterns in the Lepontine Alps, south central Switzerland, and an age of vertical movement on the Insubric fault line. Contrib. Mineral. Petrol., 92: 413-427.
Hurford, A.J. and Green, P.F., 1982. A guide to fission track dating calibration. Earth Planet. Sci. Lett., 59: 343-354.
Hurford, A.J. and Green, P.F., 1983. The zeta age calibration of fission track dating. Isot. Geosci., 1: 285-317.
Katz, H.R., 1982. Post-Beacon tectonics in the region of Amundsen and Scott Glaciers, Queen Maud Range, Transantarctic Mountains. In: C. Craddock (Editor), Antarctic Geoscience. University of Wisconsin Press, Madison, Wisc., pp. 827-834.
Kelley, S.A. and Duncan, I.J., 1986. Late Cretaceous to Middle Tertiary tectonic history of the northern Rio Grande Rift, New Mexico. J. Geophys. Res., 91: 6246-6262.
Kohn, B.P. and Eyal, M., 1981. History of uplift of the crystalline basement of Sinai and its relation to opening of the Red Sea as revealed by fission track dating of apatites. Earth Planet. Sci. Lett., 52: 129-141.
Kohn, B.P., Shagam, R., Banks, P.O. and Burkley, L.A., 1984a. Mesozoic–Pleistocene fission-tracks ages on rocks of the Venezuelan Andes and their tectonic implications. Geol. Soc. Am. Mem., 162: 365-384.
Kohn, B.P., Shagam, R. and Subieta, T., 1984b. Results and preliminary implications of sixteen-fission track ages from rocks of the western Caribbean Mountains, Venezuela. Geol. Soc. Am. Mem., 162: 415-421.
Krishnaswami, S., Lal, D., Prabhu, N. and McDougall, D., 1974. Characteristics of fission tracks in zircons: application to geochronology and cosmology. Earth Planet. Sci. Lett., 22: 51-59.
Kreuzer, A., Hohndorf, A., Heinz, L., Vetter, U., Tessensohn, F., Muller, P., Jordan, H., Harre, W. and Besang, C., 1981. K-Ar and Rb-Sr dating of igneous rocks from north Victoria Land, Antarctica. Geol. Jahrb., B41: 267-273.
Kyle, P.R., Elliot, D.H. and Sutter, J.F., 1981. Jurassic Fer-

rar Group tholeiites from the Transantarctic Mountains, Antarctica and their relationship to the initial fragmentation of Gondwana. In: M.M. Cresswell and P. Vella (Editors), Gondwana Five. A.A. Balkema, Rotterdam, pp. 283-287.

Kyle, P.R., Sutter, J.F., McIntosh, W.C., Cherry, E. and Noltimier, H., 1983. $^{40}Ar/^{39}Ar$ age spectra and palaeomagnetic measurements of Ferrar Supergroup samples from the Transantarctic Mountains, Antarctica (Abstract). In: R.L. Oliver, P.R. James and J.B. Jago (Editors), Antarctic Earth Science. Australian Academy of Science, Canberra, A.C.T., p. 242.

Laird, M.G. and Bradshaw, J.D., 1981. Permian tillites of north Victoria Land, Antarctica. In: M.J. Hambrey and W.B. Harland (Editors), Earth's Pre-Pleistocene Glacial Record. Cambridge University Press, Cambridge, pp. 237-240.

Lal, D., Rajan, R.S. and Tamhane, A.S., 1969. Chemical composition of nuclei of $Z > 22$ in cosmic rays using meteoritic minerals as detectors. Nature (London), 221: 33-37.

Laslett, G.M., Gleadow, A.J.W. and Duddy, I.R., 1984. The relationship between fission track length and density in apatite. Nucl. Tracks, 9: 29-38.

Mailhe, D., Lucazeau, F. and Vasseur, G., 1986. Uplift history of thrust belts: an approach based on fission track data and thermal modelization. Tectonophysics, 124: 177-191.

Miller, D.S. and Lakatos, S., 1983. Uplift rate of Adirondack anorthosite measured by fission track of apatite. Geology, 11: 284-286.

Naeser, C.W., 1979. Fission track dating and geologic annealing of fission tracks. In: E. Jäger and J.C. Hunziker (Editors), Lectures in Isotope Geology. Springer, New York, N.Y., pp. 154-169.

Naeser, C.W. and Faul, H., 1969. Fission track annealing in apatite and sphene. J. Geophys. Res., 74: 705-710.

Naeser, C.W., Bryant, B., Crittenden, M.D. and Sorensen, M.L., 1983. Fission-track ages of apatite in the Wasatch Mountains, Utah: An uplift study. Geol. Soc. Am. Mem., 157: 29-36.

Nelson, E.P., 1982. Post-tectonic uplift of the Cordillera Darwin orogenic complex: evidence from fission track geochronology and closing temperature-time relationships. J. Geol. Soc. London, 139: 755-761.

Parrish, R.R., 1982. Cenozoic thermal and tectonic history of the Coast Mountains of British Columbia as revealed by fission-track and geological data. Ph.D. Thesis, University of British Columbia, Vancouver, B.C., 166 pp.

Parrish, R.R., 1983. Cenozoic thermal evolution and tectonics of the Coast Mountains of British Columbia, 1. Fission-track dating, apparent uplift rates, and patterns of uplift. Tectonics, 2: 601-632.

Parrish, R.R., 1985. Some cautions which should be exercised when interpreting fission track and other data with regard to uplift rate calculations. Nucl. Tracks, 10: 425 (abstract).

Schaer, J.P., Reimer, G.M. and Wagner, G.A., 1975. Actual and ancient uplift rate in the Gotthard region, Swiss Alps: A comparison between precise leveling and fission track apatite age. Tectonophysics, 29: 293-300.

Shagam, R., Kohn, B.P., Banks, P.O., Dasch, L.E., Vargas, R., Rodriguez, G.I. and Pimentel, N., 1984. Tectonic implications of the Cretaceous-Pliocene fission track ages from rocks of the circum-Maracaibo Basin region of western Venezuela and eastern Colombia. Geol. Soc. Am. Mem., 162: 385-412.

Stump, E., Splettstoesser, J.F. and Colbert, P.V., 1982a. Northern Victoria Land Project. Antarct. J. U.S., 17: 3-4.

Stump, E., Holloway, J.R., Borg, S.G. and Lapham, K.E., 1982b. Geological investigations on early to middle Paleozoic magmatic rocks, northern Victoria Land, Antarctica. Antarct. J. U.S., 17: 17-18.

Stump, E., Holloway, J.R., Borg, S.G. and Armstrong, R.L., 1983. Discovery of a Tertiary granite pluton, northern Victoria Land. Antarct. J. U.S., 28: 17-18.

Stump, E., White, A.J.R. and Borg, S.G., 1986. Reconstruction of Australia and Antarctica: evidence from granites and recent mapping. Earth Planet. Sci. Lett., 79: 348-360.

Sturm, A. and Carryer, S.J., 1969. Geology of the region between Matusevich and Tucker Glaciers, north Victoria Land, Antarctica. N.Z. J. Geol. Geophys., 13: 408-435.

Tessensohn, F., 1984. Geological and tectonic history of the Bowers Structural Zone, north Victoria Land, Antarctica. Geol. Jahrb., B60: 371-396.

Tessensohn, F., Duphorn, K., Jordan, H., Kleinschmidt, G., Skinner, D.N.D., Vetter, U., Wright, T.O. and Wyborn, D., 1981. Geological comparison of basement units in north Victoria Land, Antarctica. Geol. Jahrb., B41: 31-88.

Wagner, G.A., 1972. The geological interpretation of fission track ages. Trans. Am. Nucl. Soc., 15: 117 (abstract).

Wagner, G.A. and Reimer, G.M., 1972. Fission track tectonics: the tectonic interpretation of fission track apatite ages. Earth Planet. Sci. Lett., 14: 263-268.

Wagner, G.A., Reimer, G.M. and Jäger, E., 1977. The cooling ages derived by apatite fission track, mica Rb-Sr, and K-Ar dating: the uplift and cooling history of the Central Alps. Inst. Geol. Mineral., Univ. of Padova, Padova, Mem. No. 30, 27 pp.

Walker, B., 1983. The Beacon Supergroup of northern Victoria Land, Antarctica. In: R.L. Oliver, P.R. James and J.B. Jago (Editors), Antarctic Earth Science. Australian Academy of Science, Canberra, A.C.T., pp. 211-214.

Weaver, S.D., Bradshaw, J.D. and Laird, M.G., 1984. Geochemistry of Cambrian volcanics of the Bowers Supergroup and implications for the Early Palaeozoic tectonic evolution of northern Victoria Land, Antarctica. Earth Planet. Sci. Lett., 68: 128-140.

Webb, P.N., 1979. Palaeogeographic evolution of the Ross

Sea sector during the Cenozoic. In: T. Nagata (Editor), Proceeding of Seminar 3 on DVDP, Tokyo. Mem. Inst. Polar Res., Spec. Iss. No. 13, pp. 206-212.

Wright, T.O., 1981. Sedimentology of the Robertson Bay Group, northern Victoria Land, Antarctica. Geol. Jahrb., B41: 127-138.

Zeitler, P.K., 1985. Cooling history of the NW Himalaya, Pakistan. Tectonics, 4: 127-151.

Zeitler, P.K., Tahirkhell, R.A.K., Naeser, C.W. and Johnson, N.M., 1982. Unroofing history of a suture zone in the Himalaya of Pakistan by means of fission track annealing ages. Earth Planet. Sci. Lett., 57: 227-240.

Zimmerman, R.A., 1977. The interpretation of apatite fission track ages with an application to the study of uplift since the Cretaceous in eastern North America. Ph.D. Thesis, University of Philadelphia, Philadelphia, Pa., 146 pp.